

Applications of the Deep Galerkin Method to Solving Partial Integro-Differential and Hamilton-Jacobi-Bellman Equations

Ali Al-Aradi^a, Adolfo Correia^b, Danilo de Frietas Naiff^c, Gabriel Jardim^d, Yuri Saporito^e

^a*Department of Statistical Sciences, University of Toronto*

^b*Instituto de Matemática Pura e Aplicada*

^c*Universidade Federal do Rio de Janeiro*

^d*Escola de Matemática Aplicada, Fundação Getulio Vargas*

^e*Escola de Matemática Aplicada, Fundação Getulio Vargas*

Abstract

We extend the Deep Galerkin Method (DGM) introduced in Sirignano and Spiliopoulos (2018) to solve a number of partial differential equations (PDEs) that arise in the context of optimal stochastic control and mean field games. First, we consider PDEs where the function is constrained to be positive and integrate to unity, as is the case with Fokker-Planck equations. Our approach involves reparameterizing the solution as the *exponential* of a neural network appropriately normalized to ensure both requirements are satisfied. This then gives rise to a partial integro-differential equation (PIDE) where the integral appearing in the equation is handled using importance sampling. Secondly, we tackle a number of Hamilton-Jacobi-Bellman (HJB) equations that appear in stochastic optimal control problems. The key contribution is that these equations are approached in their *unsimplified* primal form which includes an optimization problem as part of the equation. We extend the DGM algorithm to solve for the value function and the optimal control *simultaneously* by characterizing both as deep neural networks. Training the networks is performed by taking alternating stochastic gradient descent steps for the two functions, a technique similar in spirit to policy improvement algorithms.

Keywords: Partial differential equations; Stochastic control; Hamilton-Jacobi-Bellman equations; Deep Galerkin Method; Deep Learning; Neural Networks.

1. Introduction and Literature Review

Partial differential equations (PDEs) are ubiquitous in many areas of science, engineering, economics and finance. They are often used to describe natural phenomena and model multi-dimensional dynamical systems. In the context of finance, finding solutions to PDEs is crucial for

URL: ali.al.aradi@utoronto.ca (Ali Al-Aradi)

problems of derivative pricing, optimal investment, optimal execution, mean field games and many more. Although it is possible to obtain closed-form solutions to PDEs, more often we must resort to numerical methods for arriving at a solution. Traditional numerical approaches are presented in Burden et al. (2001), Achdou and Pironneau (2005) and Brandimarte (2013). However, many of these classical approaches - particularly grid-based approaches such as finite difference methods - are burdened with issues instability and computational cost, especially in higher dimensions. An alternative is to resort to Monte Carlo methods by appealing to the Feynman-Kac theorem to represent the solution to the PDE as an expectation and simulating to solve for the unknown function. This is primarily used for a class of linear PDEs although Monte Carlo methods for nonlinear PDEs have also been developed, e.g. E et al. (2019). In addition, there are a number of numerical algorithms based on multilevel Picard iterations that provably overcome the curse of dimensionality for general nonlinear heat equations under Lipschitz assumptions, see e.g. E et al. (2016) and Hutzenthaler et al. (2019).

In recent years, a number of approaches utilizing techniques from machine learning have been developed to overcome the curse of dimensionality faced by mesh-based methods. These approaches often involve characterizing the unknown function using a deep neural network. For example, the work of E et al. (2017) and Han et al. (2018) uses a *deep BSDE method* which reformulates the PDE of interest in terms of a backward stochastic differential equation (BSDE) by means of a nonlinear Feynman-Kac formula and then approximates the gradient of the unknown function by a neural network. An extension of this method is presented in Huré et al. (2019) and Beck et al. (2019).

In contrast, the main idea behind solving PDEs using the Deep Galerkin Method (DGM) described in the work of Sirignano and Spiliopoulos (2018) is to represent the unknown function of interest using a deep neural network. Noting that the function must satisfy a known PDE, the network is trained by minimizing losses related to the differential operator acting on the function along with any initial, terminal and/or boundary conditions the solution must satisfy. The training data for the neural network consists of different possible inputs to the function and is obtained by sampling randomly from the region on which the PDE is defined (see Figure 1.1). One of the key features of this approach is the fact that, unlike other commonly used numerical approaches such as finite difference methods, it is *mesh-free*. Simulations indicate that the Deep Galerkin Method might not suffer (as much as other numerical methods) from the curse of dimensionality associated with high-dimensional PDEs and PDE systems. A discussion of DGM and its applications can be found in Al-Arabi et al. (2018). On a related note, the work of Hutzenthaler et al. (2019) proves that deep learning-based algorithms overcome the curse of dimensionality in the numerical approximation of solutions for a class of nonlinear PDEs.

This paper addresses two perceived shortcomings of DGM. First, if the unknown function in the PDE is constrained in a certain way (for example if it is a probability density function that must be positive and integrate to unity), applying DGM does not guarantee that these constraints will be satisfied by the approximating neural network. This is true even when the constraints are directly incorporated into the loss function used to train the network. We propose a reparameterization that overcomes this difficulty.

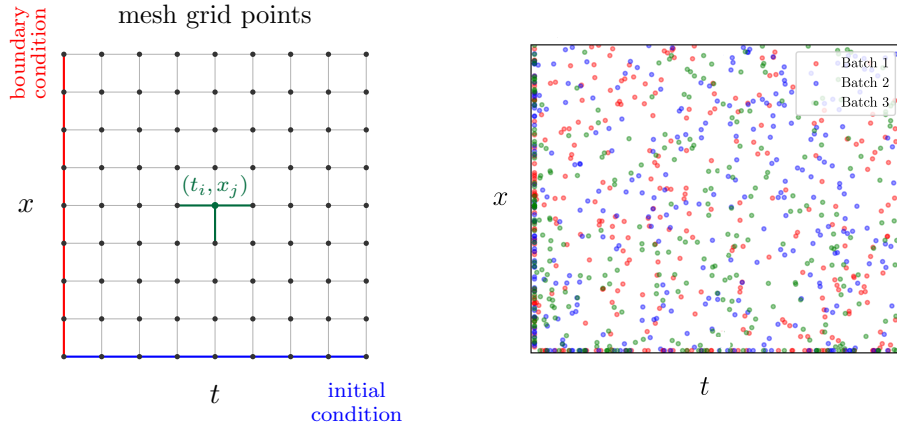


Figure 1.1: Grid-based finite differences method (left) vs. Deep Galerkin Method (right)

The second issue is tied to Hamilton-Jacobi-Bellman equations that arise in the context of stochastic control problems. Recall that such problems involve a controlled Itô process $X^u = (X_t^u)_{t \geq 0}$ satisfying the stochastic differential equation

$$dX_t^u = \mu(t, X_t^u, u_t) dt + \sigma(t, X_t^u, u_t) dW_t, \quad X_0^u = 0,$$

where $u = (u_t)_{t \geq 0}$ is a control process chosen by the controller from an admissible set \mathcal{A} . For a given control, the agent's performance criteria is:

$$H^u(t, x) = \mathbb{E} \left[\int_t^T F(s, X_s^u, u_s) ds + G(X_T^u) \mid X_t^u = x \right]$$

Assuming enough regularity, the value function $H(t, x) = \sup_{u \in \mathcal{A}} H^u(t, x)$, can be shown to satisfy a fully nonlinear PDE referred to as the Hamilton-Jacobi-Bellman (HJB) equation given by

$$\begin{cases} \partial_t H(t, x) + \sup_{u \in \mathcal{A}} \{ \mathcal{L}_t^u H(t, x) + F(t, x, u) \} = 0 \\ H(T, x) = G(x) \end{cases}$$

where the differential operator \mathcal{L}_t^u is the infinitesimal generator of the controlled process X^u . We will refer to this unsimplified form of the HJB equation as the *primal form*.

It is sometimes possible to simplify the primal form of an HJB equation by analytically solving for the optimal control in feedback form (i.e. expressed in terms of the value function and its derivatives) and substituting this quantity back into the HJB equation. This removes the optimization step that appears as the second term on the LHS of the HJB equation and leaves us with a more familiar form for the PDE that can be handled well by DGM. In fact, Sirignano and Spiliopoulos (2018) and Al-Arabi et al. (2018) both demonstrate the application of DGM to HJB equations simplified in this manner. However, sometimes it is not possible to arrive at such a simplification, and in those cases DGM would not be able to handle the optimization step. Furthermore, even in

situations where the primal form can be simplified and DGM can be successfully applied to approximate the value function, we are still left with translating the value function to the optimal control. However, we find that the error propagation in this step can lead to unsatisfactory results for the optimal control, which is arguably the main object of interest. Instead, our approach addresses both of these issues by parameterizing the unknown value function as well as the unknown optimal control as deep neural networks and training the two networks by taking alternating stochastic gradient descent steps. This is similar in spirit to the approach used in policy improvement algorithms commonly employed in reinforcement learning problems.

The remainder of this article is organized as follows: in Section 2 we review the DGM algorithm, discuss some its theoretical and implementation-related aspects and provide a simple illustrative example in the context of option pricing. Section 3 tackles the problem of PDEs with integration and positivity constraints using the Fokker-Planck equation as an example. In Section 4 we present the modified DGM algorithm and apply it to solving two HJB equations, namely the Merton problem of optimal investment and an optimal execution problem. In Section 5 we apply the modified DGM algorithm to a stochastic game which involves multiple agents leading to a system of HJB equations. Finally, in Section 6 we combine the techniques discussed in previous sections to solve a mean-field game version of the optimal execution problem, which involves a Fokker-Planck equation that is coupled with an HJB equation.

2. Review of the Deep Galerkin Method

2.1. Introduction

As mentioned in the previous section, numerical methods that are based on grids can fail when the dimensionality of the problem becomes too large. In fact, the number of points in the mesh grows exponentially in the number of dimensions which can lead to computational intractability. Furthermore, even if we were to assume that the computational cost was manageable, ensuring that the grid is set up in a way to ensure stability of the finite difference approach can be cumbersome.

With this motivation, Sirignano and Spiliopoulos (2018) propose a *mesh-free* method for solving PDEs using neural networks. The **Deep Galerkin Method** (DGM) approximates the solution to the PDE of interest with a deep neural network. With this parameterization, a loss function is set up to penalize the fitted function’s deviations from the desired differential operator and (space/time) boundary conditions. The approach takes advantage of the backpropagation algorithm to efficiently compute the differential operator while the boundary conditions are straightforward to evaluate. For the training data, the network uses points randomly sampled from the region where the function is defined and the optimization is performed using stochastic gradient descent.

The main insight of this approach lies in the fact that the training data consists of randomly sampled points in the function’s domain. By sampling mini-batches from different parts of the domain and processing these small batches sequentially, the neural network “learns” the function

without the computational bottleneck present with grid-based methods. This circumvents the curse of dimensionality which is encountered with the latter approach.

2.2. Mathematical Details

The form of the PDEs of interest are generally described as follows: let u be an unknown function of time and space defined on the region $[0, T] \times \Omega$ where $\Omega \subset \mathbb{R}^d$, and assume that u satisfies a parabolic PDE of the following form:

$$\begin{cases} (\partial_t + \mathcal{L}) u(t, \mathbf{x}) = 0, & (t, \mathbf{x}) \in [0, T] \times \Omega \\ u(0, \mathbf{x}) = u_0(\mathbf{x}), & \mathbf{x} \in \Omega & \text{(initial condition)} \\ u(t, \mathbf{x}) = g(t, \mathbf{x}), & (t, \mathbf{x}) \in [0, T] \times \partial\Omega & \text{(boundary condition)} \end{cases}$$

The goal is to approximate u with an approximating function $f(t, \mathbf{x}; \boldsymbol{\theta})$ given by a deep neural network with parameter set $\boldsymbol{\theta}$. The loss functional for the associated training problem consists of three parts:

1. A measure of how well the approximation satisfies the **differential operator**:

$$\left\| (\partial_t + \mathcal{L}) f(t, \mathbf{x}; \boldsymbol{\theta}) \right\|_{[0, T] \times \Omega, \nu_1}^2.$$

Note: parameterizing f as a neural network means that the differential operator can be computed easily using backpropagation.

2. A measure of how well the approximation satisfies the **boundary condition**:

$$\left\| f(t, \mathbf{x}; \boldsymbol{\theta}) - g(t, \mathbf{x}) \right\|_{[0, T] \times \partial\Omega, \nu_2}^2.$$

3. A measure of how well the approximation satisfies the **initial condition**:

$$\left\| f(0, \mathbf{x}; \boldsymbol{\theta}) - u_0(\mathbf{x}) \right\|_{\Omega, \nu_3}^2.$$

Note: this measure can be modified for problems with a terminal condition or extended for problems with both initial and terminal conditions.

In all three terms above the error is measured in terms of L^2 -norm, i.e. using $\|h(y)\|_{\mathcal{Y}, \nu}^2 = \int_{\mathcal{Y}} |h(y)|^2 \nu(y) dy$ with $\nu(y)$ being a density defined on the region \mathcal{Y} . Combining the three terms above gives us the cost functional associated with training the neural network:

$$L(\boldsymbol{\theta}) = \underbrace{\left\| (\partial_t + \mathcal{L}) f(t, \mathbf{x}; \boldsymbol{\theta}) \right\|_{[0, T] \times \Omega, \nu_1}^2}_{\text{differential operator}} + \underbrace{\left\| f(t, \mathbf{x}; \boldsymbol{\theta}) - g(t, \mathbf{x}) \right\|_{[0, T] \times \partial\Omega, \nu_2}^2}_{\text{boundary condition}} + \underbrace{\left\| f(0, \mathbf{x}; \boldsymbol{\theta}) - u_0(\mathbf{x}) \right\|_{\Omega, \nu_3}^2}_{\text{initial condition}}.$$

The next step is to minimize the loss functional using stochastic gradient descent. More specifically, we apply the algorithm defined in Algorithm 2.1. The description given in Algorithm 2.1 should be thought of as a general outline and the algorithm should be modified according to the particular nature of the PDE being considered.

-
-
1. Initialize the parameter set $\boldsymbol{\theta}_0$ and the learning rate α_n .
 2. Generate random samples from the domain's interior and time/spatial boundaries, i.e.
 - Generate (t_n, x_n) from $[0, T] \times \Omega$ according to ν_1
 - Generate (τ_n, z_n) from $[0, T] \times \partial\Omega$ according to ν_2
 - Generate w_n from Ω , according to ν_3
 3. Calculate the loss functional for the current mini-batch, i.e. the randomly sampled points $s_n = \{(t_n, x_n), (\tau_n, z_n), w_n\}$:
 - Compute $L_1(\boldsymbol{\theta}_n; t_n, x_n) = ((\partial_t + \mathcal{L})f(t_n, x_n; \boldsymbol{\theta}_n))^2$
 - Compute $L_2(\boldsymbol{\theta}_n; \tau_n, z_n) = (f(\tau_n, z_n; \boldsymbol{\theta}_n) - g(\tau_n, z_n))^2$
 - Compute $L_3(\boldsymbol{\theta}_n; w_n) = (f(0, w_n; \boldsymbol{\theta}_n) - u_0(w_n))^2$
 - Compute $L(\boldsymbol{\theta}_n; s_n) = L_1(\boldsymbol{\theta}_n; t_n, x_n) + L_2(\boldsymbol{\theta}_n; \tau_n, z_n) + L_3(\boldsymbol{\theta}_n; w_n)$
 4. Take a descent step at the random point s_n with Adam-based learning rates:

$$\boldsymbol{\theta}_{n+1} = \boldsymbol{\theta}_n - \alpha_n \nabla_{\boldsymbol{\theta}} L(\boldsymbol{\theta}_n; s_n)$$
 5. Repeat steps (2)-(4) until $\|\boldsymbol{\theta}_{n+1} - \boldsymbol{\theta}_n\|$ is small.
-
-

Algorithm 2.1: Deep Galerkin Method (DGM) algorithm.

It is important to notice that the problem described here is strictly an optimization problem. This is unlike typical machine learning applications where we are concerned with issues of underfitting, overfitting and generalization. Typically, arriving at a parameter set where the loss function is equal to zero would not be desirable as it suggests some form of overfitting. However, in this context a neural network that achieves this is the goal as it would be the solution to the PDE at hand. The only case where generalization becomes relevant is when we are unable to sample points everywhere within the region where the function is defined, e.g. for functions defined on unbounded domains. In this case, we would be interested in examining how well the function satisfies the PDE in those unsampled regions. The experiments conducted in Chapter 6 of Al-Arabi et al. (2018) suggest that this generalization can be quite poor.

Sirignano and Spiliopoulos (2018) also present an elegant theoretical result which is similar in

spirit to the Universal Approximation Theorem. More specifically, it is shown that deep neural network approximators converge to the solution of a class of quasilinear parabolic PDEs as the number of hidden layers tends to infinity. To state the result in more precise mathematical terms, define the following:

- $L(\boldsymbol{\theta})$, the loss functional measuring the neural network’s fit to the differential operator and boundary/initial/terminal conditions;
- \mathcal{C}^n , the class of neural networks with n hidden units;
- $f^n = \arg \min_{f \in \mathcal{C}^n} L(\boldsymbol{\theta})$, the best n -layer neural network approximation to the PDE solution.

The main result is the convergence of the neural network approximators to the *true* PDE solution:

$$f^n \rightarrow u \quad \text{as} \quad n \rightarrow \infty .$$

Further details, conditions, statement of the theorem and proofs are found in Section 7 of Sirignano and Spiliopoulos (2018). It should be noted that, similar to the Universal Approximation Theorem, this result does not prescribe a way of designing or estimating the neural network successfully.

2.3. Implementation Details

The architecture adopted by Sirignano and Spiliopoulos (2018) is similar to that of LSTMs and Highway Networks described in Hochreiter and Schmidhuber (1997) and Srivastava et al. (2015), respectively. It consists of three layers, which we refer to as **DGM layers**: an input layer, a hidden layer and an output layer, though this can be easily extended to allow for additional hidden layers.

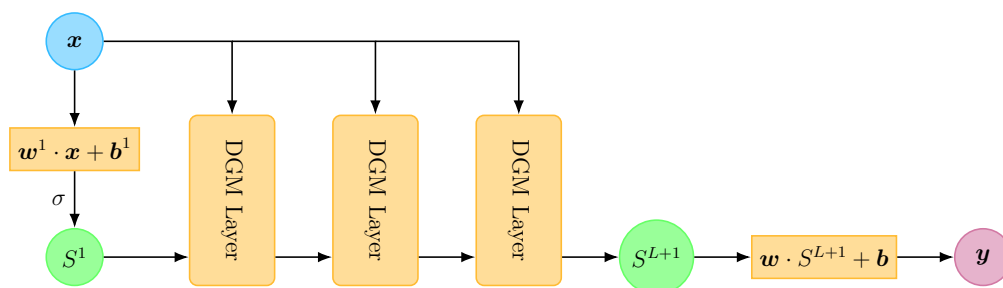


Figure 2.2: Bird’s-eye perspective of overall DGM architecture.

From a bird’s-eye perspective, each DGM layer takes as an input the original mini-batch inputs x (in our case this is the set of randomly sampled time-space points) and the output of the previous DGM layer. This process culminates with a vector-valued output y which consists of the neural network approximation of the desired function u evaluated at the mini-batch points. See Figure 2.2 for a visualization of the overall architecture.

Within a DGM layer, the mini-batch inputs along with the output of the previous layer are transformed through a series of operations that closely resemble those in Highway Networks. Below, we present the architecture in the equations along with a visual representation of a single DGM layer in Figure 2.3:

$$\begin{aligned}
S^1 &= \sigma(\mathbf{w}^1 \cdot \mathbf{x} + \mathbf{b}^1) \\
Z^\ell &= \sigma(\mathbf{u}^{z,\ell} \cdot \mathbf{x} + \mathbf{w}^{z,\ell} \cdot S^\ell + \mathbf{b}^{z,\ell}) & \ell = 1, \dots, L \\
G^\ell &= \sigma(\mathbf{u}^{g,\ell} \cdot \mathbf{x} + \mathbf{w}^{g,\ell} \cdot S^\ell + \mathbf{b}^{g,\ell}) & \ell = 1, \dots, L \\
R^\ell &= \sigma(\mathbf{u}^{r,\ell} \cdot \mathbf{x} + \mathbf{w}^{r,\ell} \cdot S^\ell + \mathbf{b}^{r,\ell}) & \ell = 1, \dots, L \\
H^\ell &= \sigma(\mathbf{u}^{h,\ell} \cdot \mathbf{x} + \mathbf{w}^{h,\ell} \cdot (S^\ell \odot R^\ell) + \mathbf{b}^{h,\ell}) & \ell = 1, \dots, L \\
S^{\ell+1} &= (1 - G^\ell) \odot H^\ell + Z^\ell \odot S^\ell & \ell = 1, \dots, L \\
f(t, \mathbf{x}; \boldsymbol{\theta}) &= \mathbf{w} \cdot S^{L+1} + \mathbf{b}
\end{aligned}$$

where \odot denotes Hadamard (element-wise) multiplication, L is the total number of layers, σ is an activation function and the \mathbf{u} , \mathbf{w} and \mathbf{b} terms with various superscripts are the model parameters.

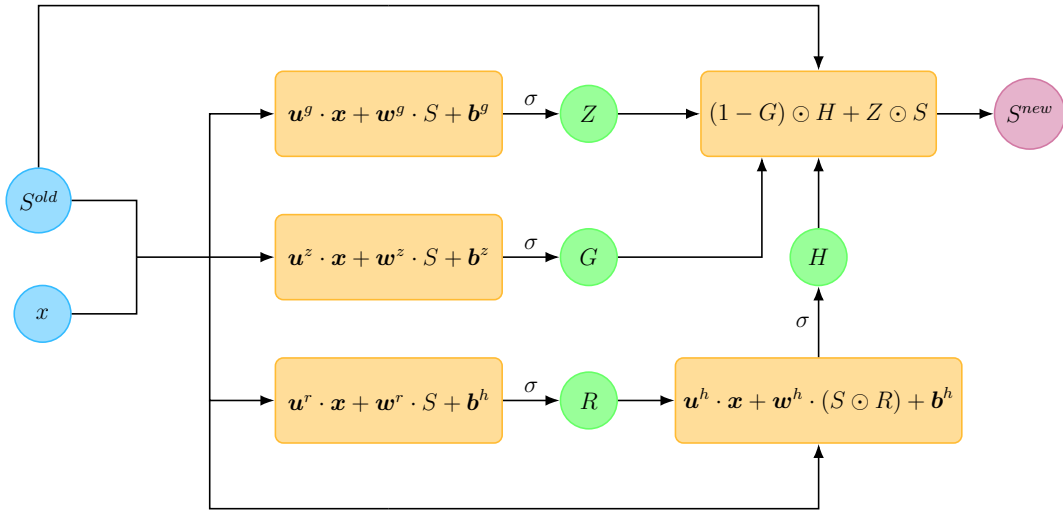


Figure 2.3: Operations within a single DGM layer.

Similar to the intuition for LSTMs, each layer produces weights based on the last layer, determining how much of the information gets passed to the next layer. In Sirignano and Spiliopoulos (2018) the authors also argue that including repeated element-wise multiplication of nonlinear functions helps capture “sharp turn” features present in more complicated functions. Note that at every iteration the original input enters into the calculations of every intermediate step, thus decreasing the probability of vanishing gradients of the output function with respect to \mathbf{x} .

Compared to a Multilayer Perceptron (MLP), the number of parameters in each hidden layer of the DGM network is roughly eight times bigger than the same number in a usual dense layer. This is the case because each DGM layer has 8 weight matrices and 4 bias vectors while the MLP

network only has one weight matrix and one bias vector (assuming the matrix/vector sizes are similar to each other). Moreover, the LSTM-like architecture of DGM networks is able to handle issues of vanishing gradients - an issue that deep MLP's may encounter - while being flexible enough to model complex functions.

As noted by Sirignano and Spiliopoulos (2018), the architecture of a neural network can be crucial to its success and clever choices of architectures, which exploit a priori knowledge about an application, can significantly improve performance. However, in our work we maintain the same architecture for the neural network, but may slightly modify the parametrization of the approximating function.

2.4. Application to Single-Name European and American Options

To illustrate some of the features of DGM, we apply this technique on a simple example: the Black-Scholes equation for derivative pricing. To recall, the Black-Scholes PDE is given by

$$\begin{cases} \partial_t g(t, x) + rx \partial_x g(t, x) + \frac{1}{2} \sigma^2 x^2 \partial_{xx} g(t, x) - r g(t, x) = 0 \\ g(T, x) = \max(x - K, 0) \end{cases}$$

where g is the unknown price function that gives the option price at time t when the underlying asset price is x and r , σ , K , and T are the risk-free rate, asset volatility, strike price and maturity time, respectively. The solution to this PDE is given by the Black-Scholes option pricing formula:

$$g(t, x) = x \Phi(d_+) - K e^{-r(T-t)} \Phi(d_-),$$

$$\text{where } d_{\pm} = \frac{\ln(x/K) + (r \pm \frac{1}{2} \sigma^2)(T-t)}{\sigma \sqrt{T-t}},$$

$\Phi(x)$ = CDF of a standard normal random variable.

For this example we take the following values for the parameters: $r = 5\%$, $\sigma = 25\%$, $T = 1$ and $K = 50$. A comparison of the DGM approximation with the analytical solution is shown in Figure 2.4 below from which we can see that the algorithm manages to recover the analytical solution to a high degree of accuracy.¹

Next, we apply the DGM approach to learning the value of American put options. The difference in this case is the inclusion of early exercise which requires us to solve a free boundary problem, namely

$$\begin{cases} \partial_t g(t, x) + rx \partial_x g(t, x) + \frac{1}{2} \sigma^2 x^2 \partial_{xx} g(t, x) - r g(t, x) = 0 & \{(t, x) : g(t, x) > G(x)\} \\ g(t, x) \geq G(x) & (t, x) \in [0, T] \times \mathbb{R} \\ g(T, x) = G(x) & x \in \mathbb{R} \end{cases}$$

¹For additional implementation-related details, the interested reader may refer to <https://github.com/alialaradi/DeepGalerkinMethod>.

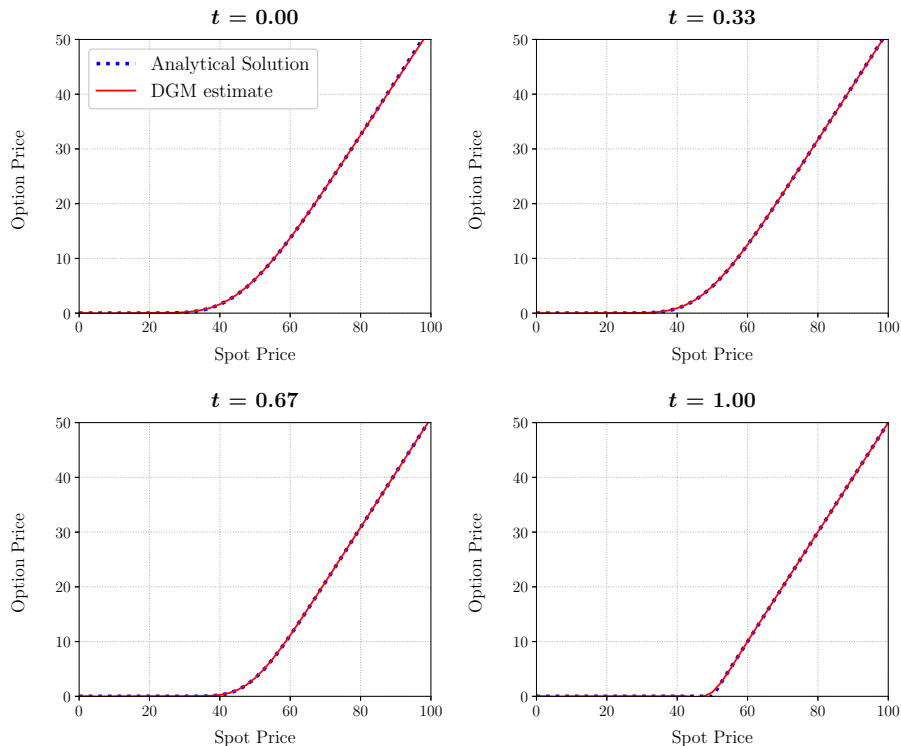


Figure 2.4: European call option prices at different times-to-maturity.

where $G(x) = \max(K - x, 0)$ is the payoff function for a put option. Once again we apply the DGM algorithm described in Figure 2.1 to the Black-Scholes equation with an added term in the loss function that accounts for the free boundary component. In particular, we apply a loss to all points that violate the condition $\{(t, x) : g(t, x) \geq G(x)\}$ via

$$\left\| \max\{-(f(t, x; \boldsymbol{\theta}) - (K - x)_+), 0\} \right\|_{[0, T] \times \Omega, \nu_1}^2.$$

Note that this deviates from the approach taken in Sirignano and Spiliopoulos (2018) which is based on acceptance/rejection of sampled points that satisfy the free boundary condition. We utilize the same parameters as the European call option case: $r = 5\%$, $\sigma = 25\%$, $T = 1$ and $K = 50$. Since there is no analytical solution for the price of American options, we compare the DGM approximation to a numerical solution obtained via finite differences. The resulting option prices are compared in Figure 2.5.

To obtain the early exercise boundary we compute the difference between the DGM-estimated put option price and the analytical prices for corresponding European puts given by the Black-Scholes formula as depicted in Figure 2.6. Since the two should be equal in the continuation region, this can be a way of indirectly obtaining the early exercise boundary. The red line is the boundary obtained by the finite difference method and we see that it is closely matched by our implied exercise boundary. The decrease in the difference between the two option prices below the boundary as time passes reflects the deterioration of the early exercise optionality in the American option.

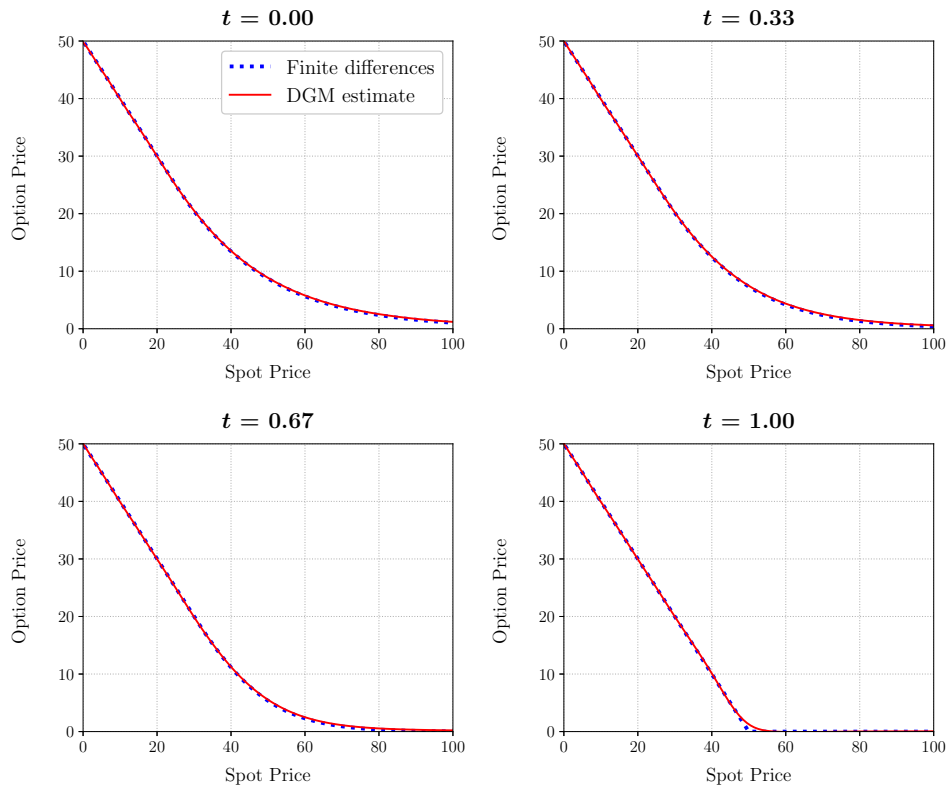


Figure 2.5: American put option prices at different times-to-maturity.

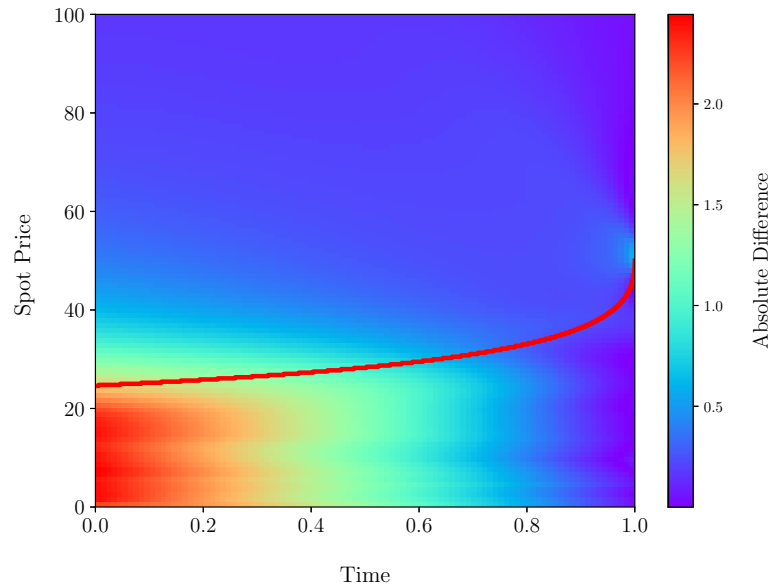


Figure 2.6: Absolute difference between DGM-estimated American put option prices and analytical solution for corresponding European put options. The red curve represents the early exercise boundary computed using finite differences.

3. PDEs with Integration and Positivity Constraints

3.1. Fokker-Planck Equations

In this section we tackle the problem of applying DGM when the unknown function in the PDE is constrained to be positive and integrate to unity. For example, this is the case when we are interested in solving a Fokker-Planck equation to obtain the time evolution of a probability density function associated with a diffusion process of interest. In particular, assume that $\mathbf{X} = (\mathbf{X}_t)_{t \geq 0}$ is an Itô process on \mathbb{R}^d with time-independent drift and diffusion coefficients, i.e.

$$d\mathbf{X}_t = \mu(\mathbf{X}_t) dt + \sigma(\mathbf{X}_t) dW_t,$$

where the initial point is a random vector \mathbf{X}_0 with distribution given by a probability density function $f(\mathbf{x})$. It follows that the probability density function of the random vector \mathbf{X}_t , denoted by $p(t, \mathbf{x})$ satisfies the PDE

$$\begin{cases} \partial_t p(t, \mathbf{x}) + \sum_{j=1}^d \partial_j (\mu_j(\mathbf{x}) p(t, \mathbf{x})) - \frac{1}{2} \sum_{i,j=1}^d \partial_{ij} (\sigma_{ij}(\mathbf{x}) p(t, \mathbf{x})) = 0 & (t, \mathbf{x}) \in \mathbb{R}_+ \times \mathbb{R}^d \\ p(0, \mathbf{x}) = f(\mathbf{x}) & \mathbf{x} \in \mathbb{R}^d \end{cases}$$

Clearly, since $p(t, \mathbf{x})$ is a probability density function we should have $p(t, \mathbf{x}) \geq 0$ for all (t, \mathbf{x}) and $\int_{\mathbb{R}^d} p(t, \mathbf{x}) d\mathbf{x} = 1$ for all t . However, a direct application of DGM to solve PDEs of this form does not guarantee that these constraints will be satisfied by the approximating neural network. This is true even when the constraints are directly incorporated into the loss function used to train the network as we will demonstrate in an example later in this section. Moreover, the incorporation of the integration constraint is extremely computationally expensive when performed at each SGD training step.

To address these issues while avoiding the computational difficulties that come with incorporating the integration penalty directly, we first reparameterize the problem by writing the density function as a normalized exponentiated function. This allows us to derive a related PDE that automatically incorporates both constraints. The result for the one-dimensional case is given in the theorem below, however this is easily extendable to the multidimensional case.

Theorem 1. *Let $X = (X_t)_{t \geq 0}$ be an Itô process satisfying the stochastic differential equation (SDE)*

$$dX_t = \mu(X_t) dt + \sigma(X_t) dW_t$$

where $\mu : \mathbb{R} \rightarrow \mathbb{R}$ and $\sigma : \mathbb{R} \rightarrow \mathbb{R}^+$ are time-independent functions. Furthermore, let $p(t, x)$ be the probability density function associated with X_t i.e. $\mathbb{P}(X_t \in A) = \int_A p(t, x) dx$ and define the function $u(t, x)$ via

$$p(t, x) = \frac{e^{-u(t,x)}}{\int_{\mathbb{R}} e^{-u(t,y)} dy}.$$

Then u satisfies the PDE

$$\begin{cases} \partial_t u - \partial_x \mu + \mu(x) \partial_x u - \frac{1}{2} \left[\partial_{xx} \sigma^2 - 2 \partial_x \sigma^2 \partial_x u + \sigma^2(x) \left((\partial_x u)^2 - \partial_{xx} u \right) \right] - \frac{\int_{\mathbb{R}} e^{-u(t,x)} \partial_t u \, dx}{\int_{\mathbb{R}} e^{-u(t,x)} \, dx} = 0, & (t, x) \in \mathbb{R}_+ \times \mathbb{R} \\ u(0, x) = -\ln(f(x) c(0)), \end{cases}$$

where $c(0) = \int_{\mathbb{R}} e^{-u(0,x)} \, dx$.

Proof. See Appendix A. ■

This new equation is a non-linear partial integro-differential equation (PIDE). To handle the integral term and avoid the costly operation of numerically integrating at each step, we notice that since we have uniformly sampled $\{t_j\}_{j=1}^{N_t}$ from $[0, T]$ and $\{x_k\}_{k=1}^{N_x}$ from $[x_{min}, x_{max}]$ at each epoch as part of the DGM algorithm, we can use **importance sampling** to approximate the integral for each t_j . That is,

$$\int_{\mathbb{R}} \partial_t u(t_j, x) \frac{e^{-u(t_j, x)}}{\int_{\mathbb{R}} e^{-u(t_j, y)} \, dy} \, dx \approx \sum_{k=1}^{N_x} \partial_t u(t_j, x_k) w(x_k),$$

where

$$w(x_k) = \frac{e^{-u(t_j, x_k)}}{\sum_{i=1}^{N_x} e^{-u(t_j, x_i)}}.$$

Note that this procedure can be adapted to other PDEs with similar constraints and to the multidimensional setting. Applying the DGM algorithm to this PDE to solve for $u(t, x)$ and then translating the output back to the density function $p(t, x)$ guarantees that the resulting approximation will remain positive and integrate to unity.

3.2. Application to Ornstein-Uhlenbeck Processes with Random Gaussian Start

As an example, let $X = (X_t)_{t \geq 0}$ be an Ornstein-Uhlenbeck (OU) process with parameters κ, θ and σ being the reversion rate, reversion level and volatility, respectively. That is, X satisfies the SDE

$$dX_t = \kappa(\theta - X_t) \, dt + \sigma \, dW_t.$$

Assume further that the process starts at a random point drawn from a normal distribution with mean m and variance v^2 , i.e. $X_0 \sim \mathcal{N}(m, v^2)$. The conditional distribution of X_t given the starting point X_0 is

$$X_t | X_0 \sim \mathcal{N} \left(X_0 e^{-\kappa t} + \theta (1 - e^{-\kappa t}), \frac{\sigma^2}{2\kappa} (1 - e^{-2\kappa t}) \right).$$

It is straightforward to show using a conjugate prior argument that the marginal distribution of X_t is also normal. In particular, we have

$$X_t \sim \mathcal{N} \left(\underbrace{m e^{-\kappa t} + \theta (1 - e^{-\kappa t})}_{M_t}, \underbrace{\frac{\sigma^2}{2\kappa} (1 - e^{-2\kappa t}) + v^2 e^{-2\kappa t}}_{V_t^2} \right).$$

Moreover, according to the Fokker-Planck equation, the probability density function $p(t, x)$ associated with X_t satisfies the PDE

$$\begin{cases} \partial_t p(t, x) - \kappa p(t, x) + \kappa(\theta - x) \partial_x p(t, x) - \frac{1}{2} \sigma^2 \partial_{xx} p(t, x) = 0 & (t, x) \in \mathbb{R}_+ \times \mathbb{R} \\ p(0, x) = \frac{1}{\sqrt{2\pi v}} \exp \left[-\frac{1}{2} \left(\frac{x - m}{v} \right)^2 \right] \end{cases}$$

From the marginal distribution of X_t given above we can deduce that the solution to this PDE is

$$p(t, x) = \frac{1}{\sqrt{2\pi V_t}} \exp \left[-\frac{1}{2} \left(\frac{x - M_t}{V_t} \right)^2 \right]$$

and we can use this result to assess the accuracy of our numerical solutions to the aforementioned PDE.

As mentioned earlier, directly applying the DGM algorithm to solve the Fokker-Planck equation does not guarantee that the positivity and integration constraints will be satisfied. This is true even when the constraints are directly incorporated into the loss function used to train the network. To demonstrate this we apply the DGM algorithm on the Fokker-Planck equation for the OU process with a random Gaussian starting point. We add an additional term in the loss function (besides the usual terms for the differential operator and the initial condition) to reflect the non-negativity constraint, namely (following the notation of Figure 2.1):

$$L_{pos}(\boldsymbol{\theta}_n; t_n, x_n) = \max\{-f(\boldsymbol{\theta}_n; t_n, x_n), 0\}$$

We did not include a penalty term to force the integral of the approximating function to equal one since it proved to be too computationally expensive due to the fact that a numerical integration procedure had to run at each step of the network training phase. Instead, we opted for normalizing the density function after the estimation was completed. Figure 3.1 shows the results of this approach for the parameters $\kappa = 0.5$, $\theta = 0$, $\sigma = 2$ and $T = 1$. The plots show that, while the initial condition was somewhat well-approximated, the fitted distributions had issues around the tails of the distribution at later times and that the Gaussian bell shape was not conserved across time.

Using the alternative approach we apply Theorem 1 to obtain the PDE that the function u must satisfy, which is

$$\begin{cases} \partial_t u + \kappa + \kappa(\theta - x) \partial_x u + \frac{\sigma^2}{2} \left((\partial_x u)^2 - \partial_{xx} u \right) - \int_{\mathbb{R}} \frac{e^{-u(t,x)}}{\int_{\mathbb{R}} e^{-u(t,y)} dy} \partial_t u(t, x) dx = 0 & (t, x) \in \mathbb{R}_+ \times \mathbb{R} \\ u(0, x) = \frac{1}{2} \left(\frac{x - \mu}{v} \right)^2 \end{cases}$$

The results of the modified approach are given in Figure 3.2 and the plots show a marked improvement over the direct implementation of DGM to this problem.

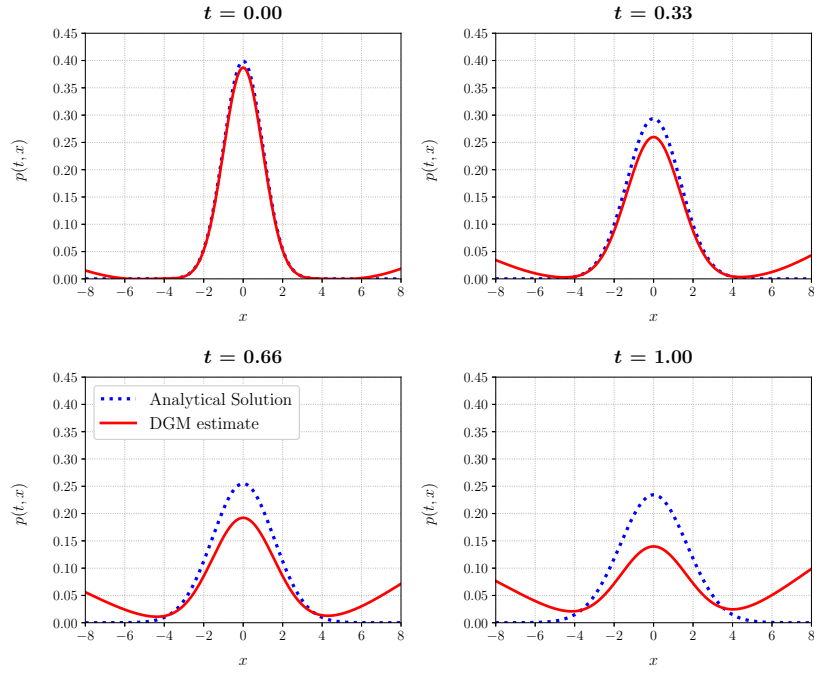


Figure 3.1: Distribution of OU process X_t with random Gaussian starting point at different times.

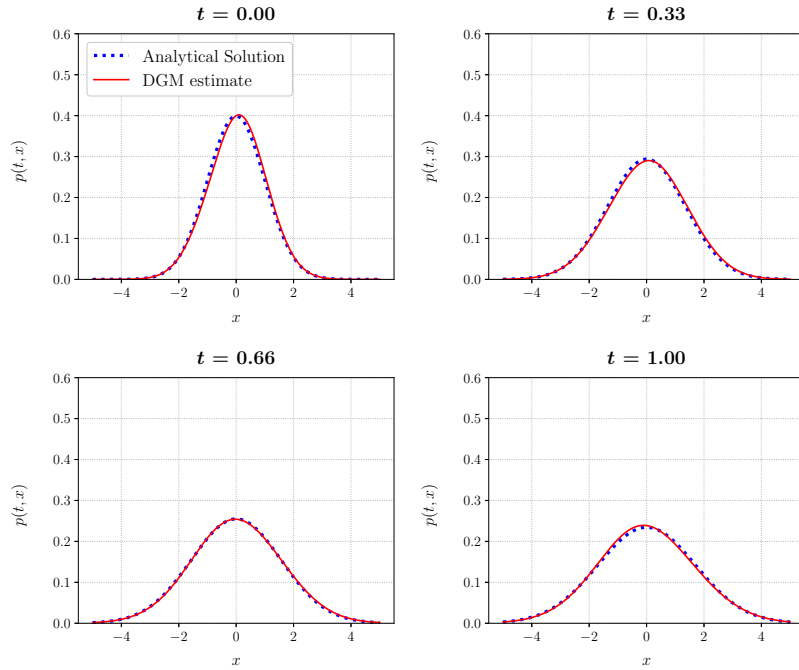


Figure 3.2: Distribution of OU process X_t with random Gaussian starting point at different times using the modified approach.

4. Hamilton-Jacobi-Bellman Equations

In this section we consider applying a modified version of DGM to solving HJB equations in their primal form, i.e. in the form

$$\begin{cases} \partial_t H(t, \mathbf{x}) + \underbrace{\sup_{u \in \mathcal{A}} \{ \mathcal{L}_t^u H(t, \mathbf{x}) + F(t, \mathbf{x}, u) \}}_{\text{optimization/first-order condition}} = 0 \\ H(T, \mathbf{x}) = G(\mathbf{x}) \end{cases}$$

In the PDE above we are interested in solving for the unknown value function H and the unknown optimal feedback control u^* both of which are defined on the region $[0, T] \times \Omega$ where $\Omega \subset \mathbb{R}^d$. As discussed in the outset, it would be difficult to apply DGM directly to an HJB equation of this nature due to the optimization component that appears in the PDE. The typical approach for a naïve application of DGM would be to solve for the optimal control in feedback form, substitute it back into the PDE and eliminate the optimization component, making it possible to apply DGM directly. However, such a simplification is not always feasible. Moreover, solving for the value function using DGM and then translating the output to obtain the optimal control may lead to unsatisfactory results due to possible instabilities that arise from the dependence of the optimal control on the derivatives of the value function.

The alternative we propose to overcome these difficulties is a modification of the DGM algorithm inspired by the policy improvement algorithm (PIA) used in reinforcement learning which allows us to obtain a numerical solution for both the value function and the optimal control simultaneously. We begin by presenting a brief summary of PIA. Given a control in feedback form u , denote $\mathcal{L}^u H(t, \mathbf{x}) = \mathcal{L}^{u(t, \mathbf{x})} H(t, \mathbf{x})$ and let u_0 be an initial control. Then for $n \geq 0$ the algorithm involves alternating between two steps:

1. Find a classical solution to the linear PDE

$$\begin{cases} \partial_t H^{u_n}(t, \mathbf{x}) + \mathcal{L}^{u_n} H^{u_n}(t, \mathbf{x}) + F(t, \mathbf{x}, u_n(t, \mathbf{x})) = 0 \\ H^{u_n}(T, \mathbf{x}) = G(\mathbf{x}) \end{cases} \quad (4.1)$$

for the fixed control u_n .

2. Compute the policy improvement

$$u_{n+1}(t, \mathbf{x}) = \arg \max_{u \in \mathcal{A}} \left\{ \mathcal{L}^u H^{u_n}(t, \mathbf{x}) + F(t, \mathbf{x}, u) \right\} \quad (4.2)$$

for the fixed value function H^{u_n} .

The convergence of PIA has been studied in several frameworks, e.g. Jacka and Mijatović (2017) and other references therein. In the case of stochastic control problems for continuous-time processes we have the following result:

Theorem 2. *Under the assumptions stated in Jacka and Mijatović (2017), we have*

$$H^{u_n}(t, \mathbf{x}) \leq H^{u_{n+1}}(t, \mathbf{x}) \quad \text{and} \quad \lim_{n \rightarrow +\infty} H^{u_n}(t, \mathbf{x}) = H(t, \mathbf{x}).$$

Moreover, there exists a sub-sequence $(u_{n_k})_{k \in \mathbb{N}}$ such that $u_{n_k} \rightarrow u^*$ uniformly on compacts.

4.1. Modified Deep Galerkin Method for HJB Equations (DGM-PIA)

The main idea of the algorithm proposed here is to combine the DGM and PIA algorithms. The modification to the DGM approach involves approximating the value function H and the optimal control u^* with functions $f(t, \mathbf{x}; \boldsymbol{\theta}^H)$ and $g(t, \mathbf{x}; \boldsymbol{\theta}^u)$ given by two deep neural networks with parameter sets $\boldsymbol{\theta}^H$ and $\boldsymbol{\theta}^u$. Since there are two optimization problems - one corresponding to the first-order equation, the other to the PDE satisfied by the value function - we define two loss functionals associated with training f and g . The first loss functional addresses the differential operator and the terminal condition related to the PDE of the value function:

$$L_H(\boldsymbol{\theta}^H) = \underbrace{\left\| \left(\partial_t + \mathcal{L}^{g(t, \mathbf{x}; \boldsymbol{\theta}^u)} \right) f(t, \mathbf{x}; \boldsymbol{\theta}^H) + F(t, \mathbf{x}, g(t, \mathbf{x}; \boldsymbol{\theta}^u)) \right\|_{[0, T] \times \Omega, \nu_1}^2}_{\text{differential operator}} + \underbrace{\left\| f(T, \mathbf{x}; \boldsymbol{\theta}^H) - G(\mathbf{x}) \right\|_{\Omega, \nu_2}^2}_{\text{terminal condition}}$$

The second is associated with the auxiliary optimization problem that arises from the first-order condition term:

$$L_u(\boldsymbol{\theta}^u) = - \underbrace{\int_{[0, T] \times \Omega} \left[\mathcal{L}^{g(t, \mathbf{x}; \boldsymbol{\theta}^u)} f(t, \mathbf{x}; \boldsymbol{\theta}^H) + F(t, \mathbf{x}, g(t, \mathbf{x}; \boldsymbol{\theta}^u)) \right] d\nu_1(t, \mathbf{x})}_{\text{first-order condition}}$$

This latter term is related to the policy improvement equation (4.2), however it addresses this optimization in an average sense over the domain and sampled points rather than pointwise as in (4.2). In order to minimize the two loss functionals, we apply stochastic gradient descent in an alternating manner. That is, we take one SGD step for $\boldsymbol{\theta}^H$, then fixing this parameter set value take one SGD step for $\boldsymbol{\theta}^u$. The modified DGM algorithm is defined in detail in Algorithm 4.1. As is the case with the original DGM algorithm, the description given in Algorithm 4.1 should be thought of as a general outline that can be modified according to the particular nature of the HJB problem being considered.

Remark. A similar combination of PIA and neural networks was studied for a different class of PDE problems, namely semilinear Hamilton-Jacobi-Bellman-Isaacs (HJBI) boundary value problems, in Ito et al. (2019). Their algorithm, named *inexact PIA*, considers a neural network approximation of the linear PDE (4.1). The authors then analyze the convergence of this algorithm under this class of PDEs and prove its superlinear convergence.

In the subsequent sections we will consider various optimal control problems and numerically solve the associated HJB equations using the DGM-PIA algorithm and the naïve application of the DGM algorithm to HJB equations discussed earlier in this section. In each application we will present a very brief description of the problem; for more details the reader is referred to the original papers or to the report by Al-Aradi et al. (2018) for more complete descriptions and summaries.

-
1. Initialize parameter sets for the value function θ_0^H and optimal control θ_0^u and the learning rate α_n .
 2. Generate random samples from the domain's interior and time/spatial boundaries, i.e.
 - **Generate** (t_n, x_n) from $[0, T] \times \Omega$ according to ν_1
 - **Generate** (τ_n, z_n) from $[0, T] \times \partial\Omega$ according to ν_2
 3. Calculate the value function loss functional for the current mini-batch, i.e. the randomly sampled points $s_n = \{(t_n, x_n), (\tau_n, z_n), w_n\}$:
 - **Compute** $L_{H,1}(\theta_n^H; t_n, x_n) = [(\partial_t + \mathcal{L}^{g(t_n, x_n; \theta_n^u)}) f(t_n, x_n; \theta_n^H) + F(t_n, x_n, g(t_n, x_n; \theta_n^u))]^2$
 - **Compute** $L_{H,2}(\theta_n^H; \tau_n, z_n) = (f(\tau_n, z_n; \theta_n^H) - G(\tau_n, z_n))^2$
 - **Compute** $L_H(\theta_n^H; s_n) = L_{H,1}(\theta_n^H; t_n, x_n) + L_{H,2}(\theta_n^H; \tau_n, z_n)$
 4. Take a descent step at the random point s_n with Adam-based learning rates:

$$\theta_{n+1}^H = \theta_n^H - \alpha_n \nabla_{\theta} L_H(\theta_n^H; s_n)$$

5. Calculate the optimal control loss functional for the current mini-batch:
 - **Compute** $L_u(\theta_n^u; s_n) = -[\mathcal{L}^{g(t_n, x_n; \theta_n^u)} f(t_n, x_n; \theta_n^H) + F(t_n, x_n, g(t_n, x_n; \theta_n^u))]$
6. Take a descent step at the random point s_n with Adam-based learning rates:

$$\theta_{n+1}^u = \theta_n^u - \alpha_n \nabla_{\theta} L_u(\theta_n^u; s_n)$$

7. Repeat steps (2)-(6) until $\|\theta_{n+1}^H - \theta_n^H\|$ and $\|\theta_{n+1}^u - \theta_n^u\|$ are small.
-

Algorithm 4.1: *Modified Deep Galerkin Method for HJB Equations (DGM-PIA) algorithm.*

4.2. Merton Problem

In this section we apply the modified DGM approach to solving the Merton problem with exponential utility. Recall that in the Merton problem, an agent chooses the proportion of their wealth that they wish to invest in a risky asset and a risk-free asset through time. They seek to maximize the expected utility of terminal wealth at the end of their investment horizon; see Merton (1969) for the investment-consumption problem and Merton (1971) for extensions in a number of directions. The HJB equation associated with this stochastic control problem is

$$\begin{cases} \partial_t H + \sup_{\pi \in \mathcal{A}} \left\{ ((\pi(\mu - r) + rx) \partial_x + \frac{1}{2} \sigma^2 \pi^2 \partial_{xx} + (\mu - r)S \partial_S + \frac{1}{2} \sigma^2 S^2 \partial_{SS} + \sigma \pi \partial_{xS}) H \right\} = 0 \\ H(T, x, S) = U(x) \end{cases} \quad (4.3)$$

where the model's parameters are μ , σ and r , the asset's drift and volatility and the risk-free rate, respectively. The proportion of wealth invested in the risky asset, π , is the agent's control. The

state variables x and S are the agent's wealth and the price of the risky asset and $U(x)$ is the agent's utility function. Noticing that we select an ansatz for H that is independent of S , the HJB equation above could be simplified to

$$\begin{cases} \partial_t H + rx \partial_x H - \frac{\lambda^2 (\partial_x H)^2}{2 \partial_{xx} H} = 0 \\ H(T, x) = U(x) \end{cases} \quad (4.4)$$

where $\lambda = \frac{\mu - r}{\sigma}$ is the market price of risk; see Section 5.3 of Cartea et al. (2015).

If we assume an exponential utility function with risk preference parameter γ , that is $U(x) = -e^{-\gamma x}$, then the value function and the optimal control can be obtained in closed-form:

$$H(t, x) = -\exp \left[-x\gamma e^{r(T-t)} - \frac{\lambda^2}{2}(T-t) \right] \quad (4.5a)$$

$$\pi_t^* = \frac{\lambda}{\gamma\sigma} e^{-r(T-t)}. \quad (4.5b)$$

We apply DGM to (4.4) and DGM-PIA to (4.3) with parameters $r = 0.02$, $\mu = 0.05$, $\sigma = 0.25$, $\gamma = 1$ and $T = 1$. The estimated value function and optimal control as well as the relative and absolute errors compared to the analytical solution in (4.5) are given in Figures 4.2 to 4.5. It is noteworthy that the DGM-PIA algorithm gives more stable optimal control as shown in Figure 4.2.

4.3. Optimal Execution

HJB equations feature prominently in the algorithmic trading literature, such as in the classical work of Almgren and Chriss (2001) and more recently Cartea and Jaimungal (2015) and Cartea and Jaimungal (2016) to name a few. In this section, we discuss a simple algorithmic trading problem with an investor that wishes to liquidate an inventory of shares but is subject to linear price impact and faces terminal and running inventory penalties. We omit a detailed discussion of the problem and refer the interested reader to Chapter 6 of Cartea et al. (2015) for additional details and for other optimal execution problems. For our purposes, we are interested in the HJB equation that arises in the context of this problem which is given by

$$\begin{cases} (\partial_t + \frac{1}{2}\sigma^2 \partial_{SS})H - \phi q^2 + \sup_{\nu \in \mathcal{A}} \left\{ (\nu(S - \kappa\nu)\partial_x - b\nu \partial_S - \nu\partial_q) H \right\} = 0 \\ H(t, x, S, q) = x + Sq - \alpha q^2 \end{cases} \quad (4.6)$$

where H is the unknown value function; ν is the agent's (liquidation) trading rate; the state variables x , S and q correspond to the investor's cash, the asset price and the investor's inventory; σ is the asset's volatility; k and b are temporary and permanent price impact parameters; ϕ and α are running and terminal inventory penalty parameters. We start by carefully choosing the ansatz

$$H(t, x, S, q) = x + qS + h(t, q).$$

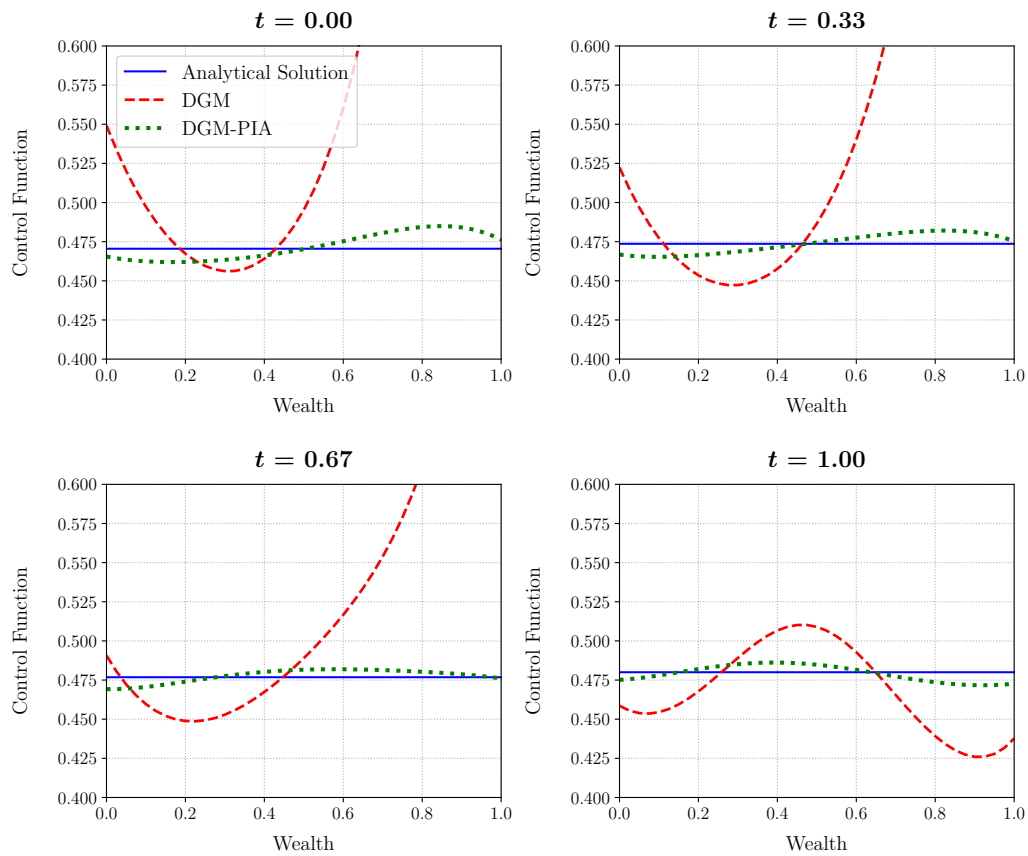


Figure 4.2: Optimal control of the Merton problem at different times.

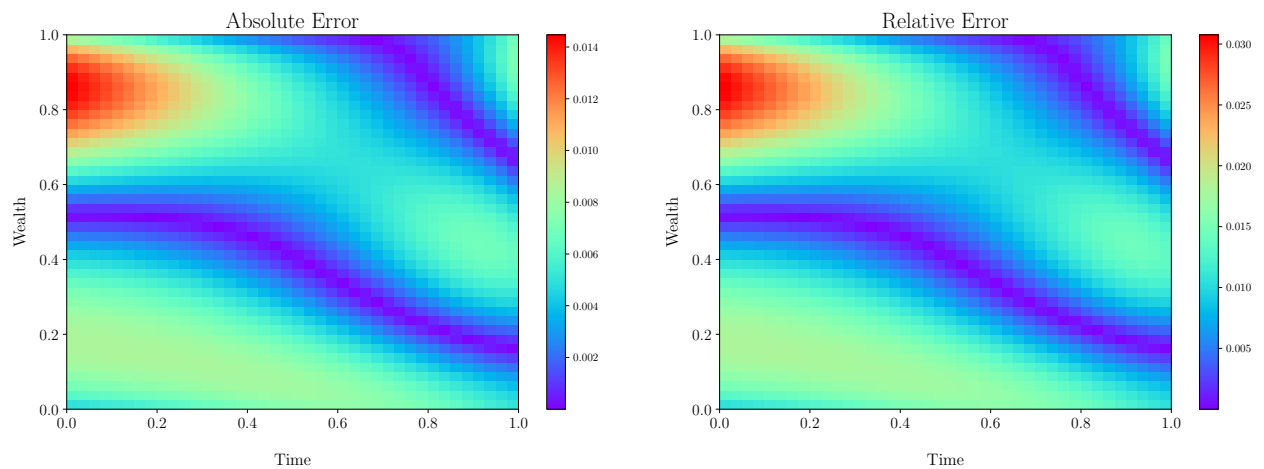


Figure 4.3: Absolute (left panel) and relative (right panel) error in the optimal control of the Merton problem compared to the analytical solution.

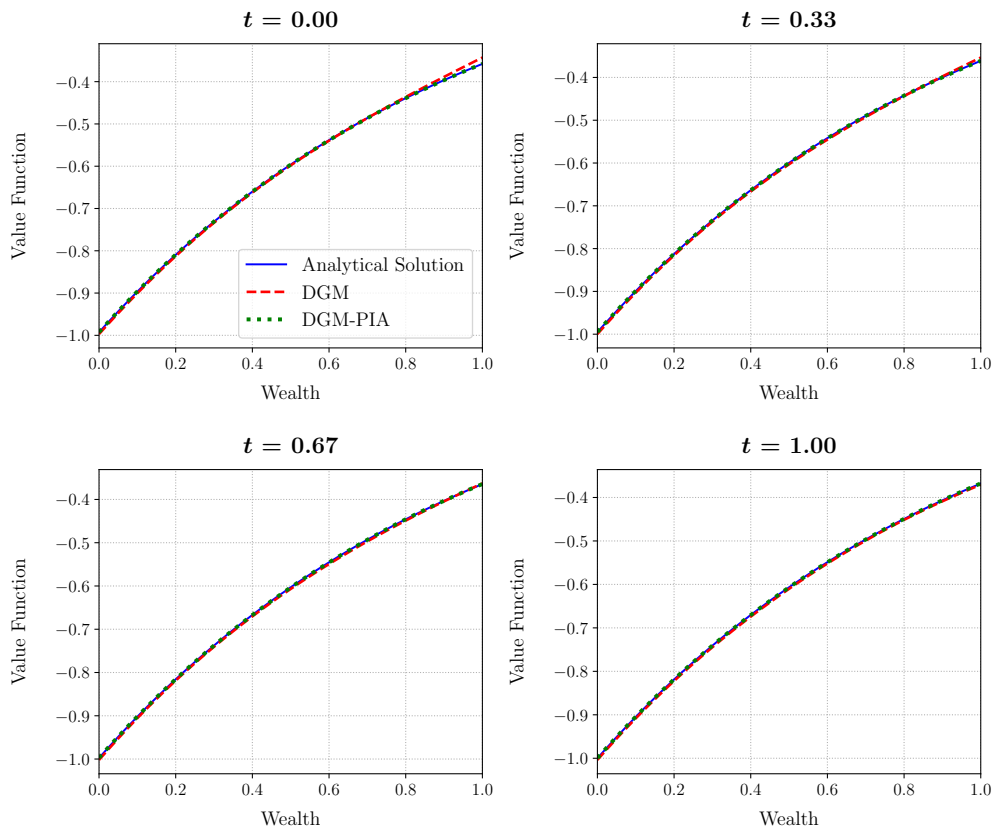


Figure 4.4: Value function of the Merton problem at different times.

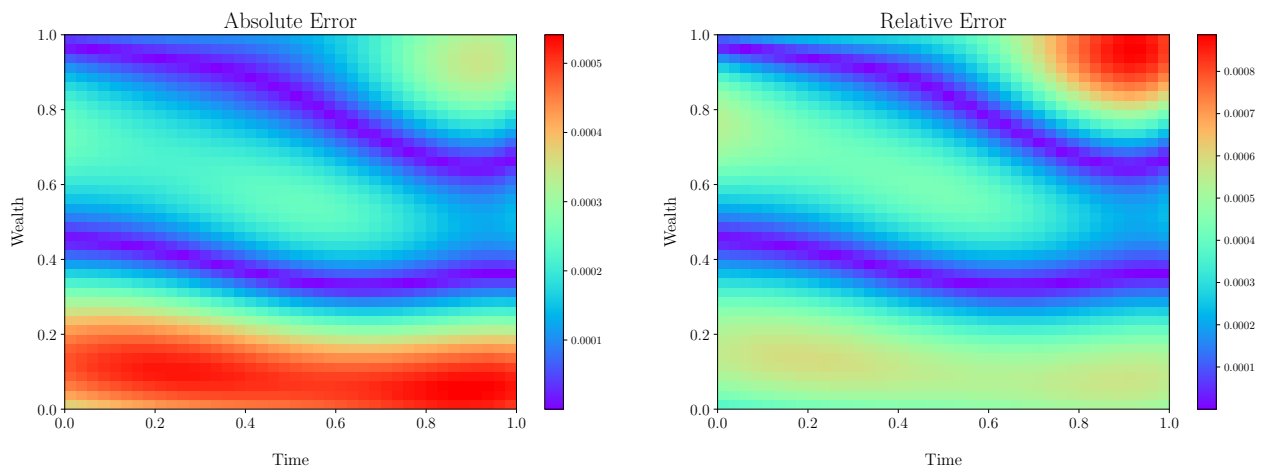


Figure 4.5: Absolute (left panel) and relative (right panel) error in the value function of the Merton problem compared to the analytical solution.

The PDE (4.6) becomes

$$\begin{cases} \partial_t h - \phi q^2 + \sup_{\nu \in \mathcal{A}} \left\{ \nu(-bq - \kappa\nu - \partial_q h) \right\} = 0 \\ h(t, q) = -\alpha q^2, \end{cases} \quad (4.7)$$

which could be simplified to

$$\begin{cases} \partial_t h - \phi q^2 + \frac{(bq + \partial_q h)^2}{4\kappa} = 0 \\ h(t, q) = -\alpha q^2 \end{cases} \quad (4.8)$$

We can then solve for the value function and optimal control:

$$H(t, x, S, q) = x + qS + \left(g(t) - \frac{b}{2}\right) q^2 \quad (4.9a)$$

$$\nu_t^* = \gamma \frac{\zeta e^{\gamma(T-t)} + e^{-\gamma(T-t)}}{\zeta e^{\gamma(T-t)} - e^{-\gamma(T-t)}} q_t^* \quad (4.9b)$$

$$\text{where } g(t) = \sqrt{\kappa\phi} \frac{1 + \zeta e^{2\gamma(T-t)}}{1 - \zeta e^{2\gamma(T-t)}}, \quad \gamma = \sqrt{\frac{\phi}{\kappa}}, \quad \zeta = \frac{\alpha - \frac{1}{2}b + \sqrt{\kappa\phi}}{\alpha - \frac{1}{2}b - \sqrt{\kappa\phi}}.$$

Now, we apply the DGM-PIA and DGM algorithms to the PDEs (4.7) and (4.8), respectively, with parameters $k = 0.01$, $b = 0.001$, $\phi = 0.1$, $\alpha = 0.1$ and $T = 1$. The estimated value function and optimal control as well as the relative and absolute errors compared to the analytical solutions are given in Figures 5.1 to 5.4. As in the previous example, the modified DGM gives a more stable optimal control, mainly around $q = 0$, as demonstrated in Figure 5.1.

5. Systems of HJB Equations

5.1. Systemic Risk

The next application we consider is based on the work of Carmona et al. (2015) on systemic risk which studies instability in a market where a number of banks are borrowing and lending with the central bank. Each player in this stochastic game aims to be at or around the average monetary reserve level across the economy.

We will focus on the system of HJB equations that characterize the optimal behavior of players and refer the interested reader to the original paper for additional details. The unsimplified HJB equation for agent $i \in \{1, \dots, n\}$ is

$$\begin{cases} \partial_t V^i + \inf_{\alpha^i} \left\{ \sum_{j=1}^N [a(\bar{x} - x^j) + \alpha^j] \partial_j V^i + \frac{\sigma^2}{2} \sum_{j,k=1}^N (\rho^2 + \delta_{jk}(1 - \rho^2)) \partial_{jk} V^i \right. \\ \left. + \frac{(\alpha^i)^2}{2} - q\alpha^i(\bar{x} - x^i) + \frac{\epsilon}{2} (\bar{x} - x^i)^2 \right\} = 0 \\ V^i(T, \mathbf{x}) = \frac{\epsilon}{2} (\bar{x} - x^i)^2 \end{cases} \quad (5.1)$$

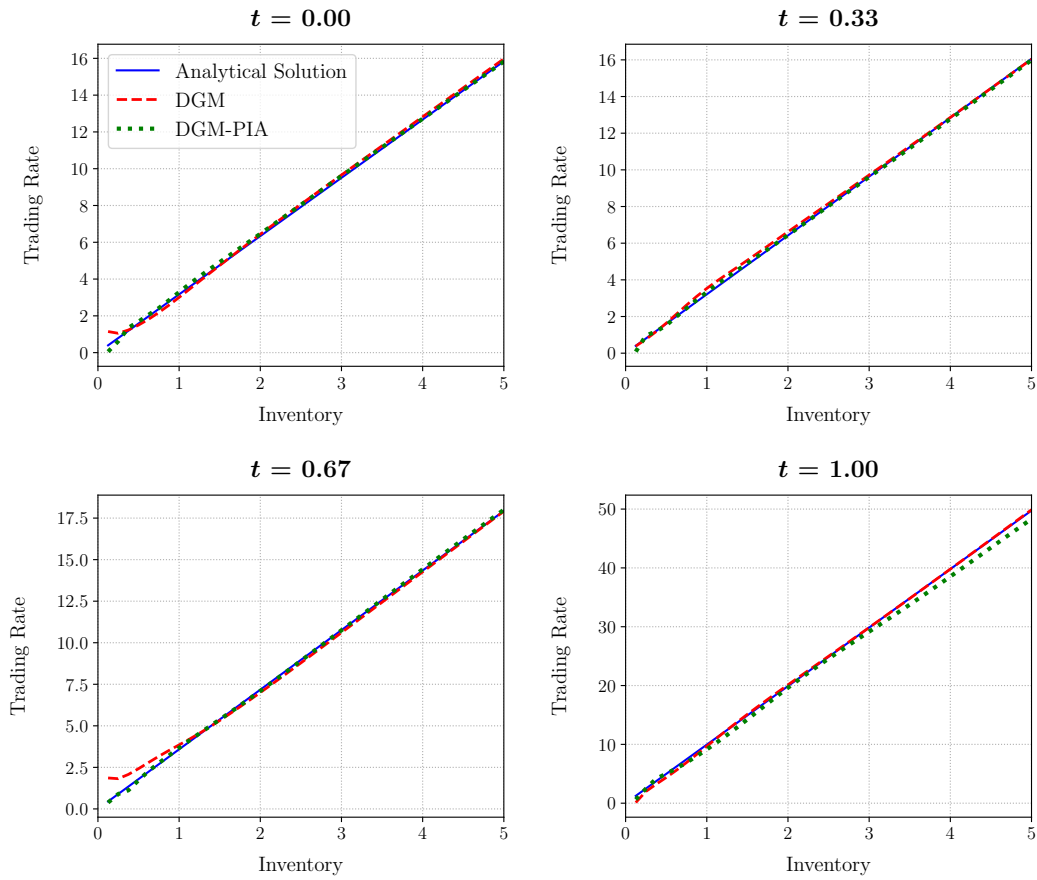


Figure 5.1: Optimal control for the optimal execution problem at different times.

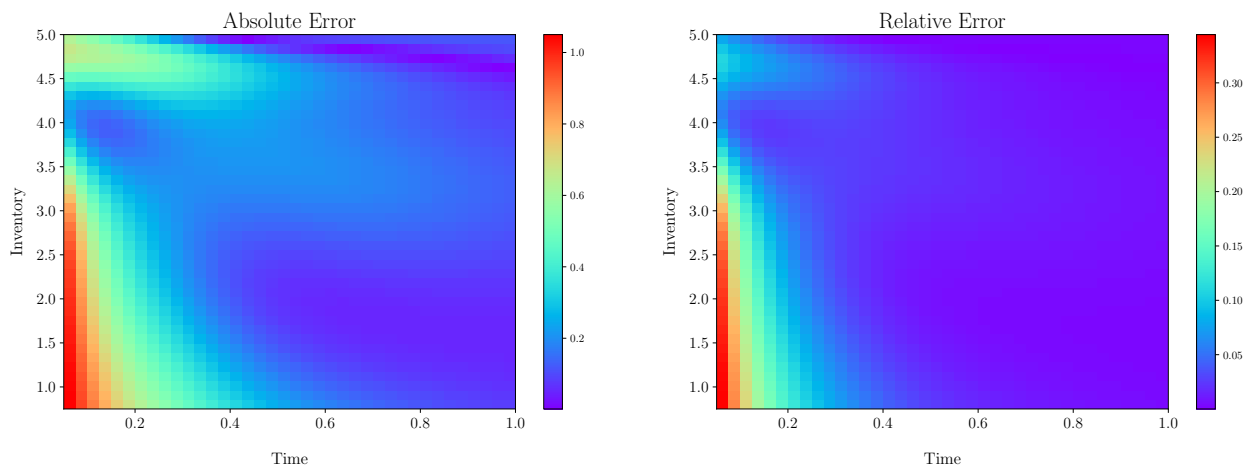


Figure 5.2: Absolute (left panel) and relative (right panel) error in the optimal control of the optimal execution problem compared to the analytical solution.

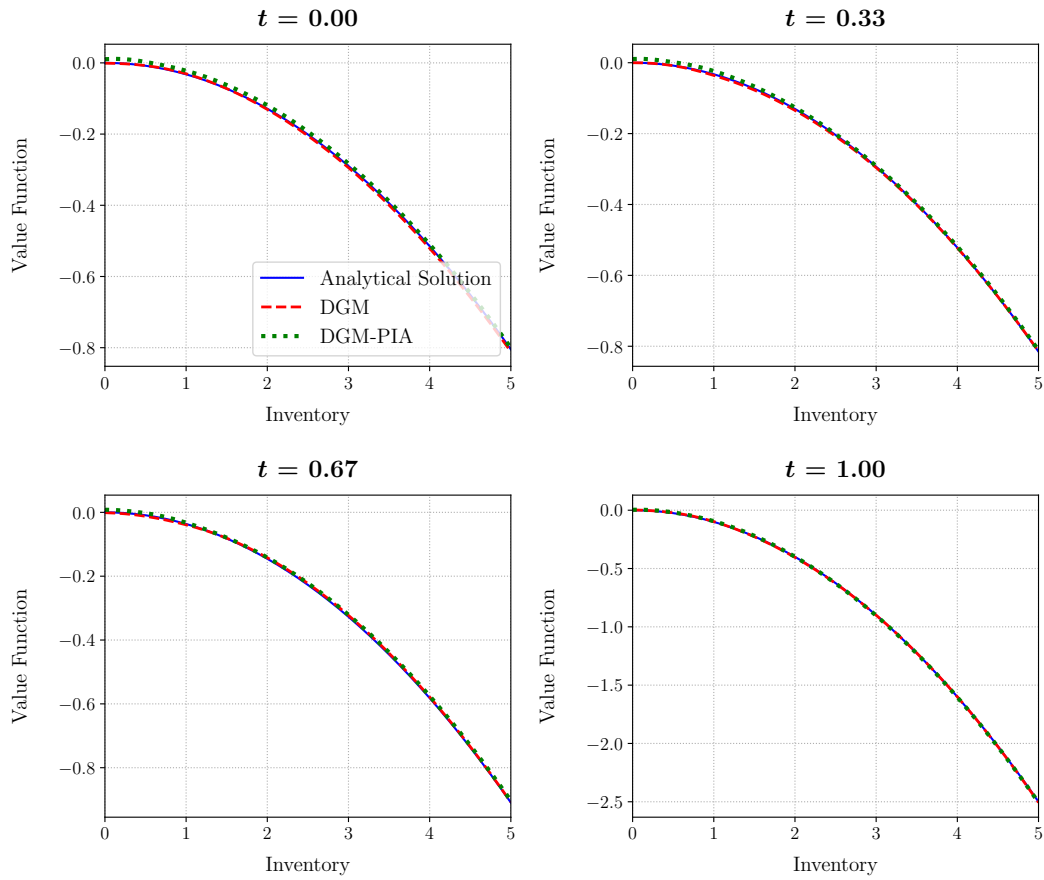


Figure 5.3: Value function of the optimal execution problem control at different times.

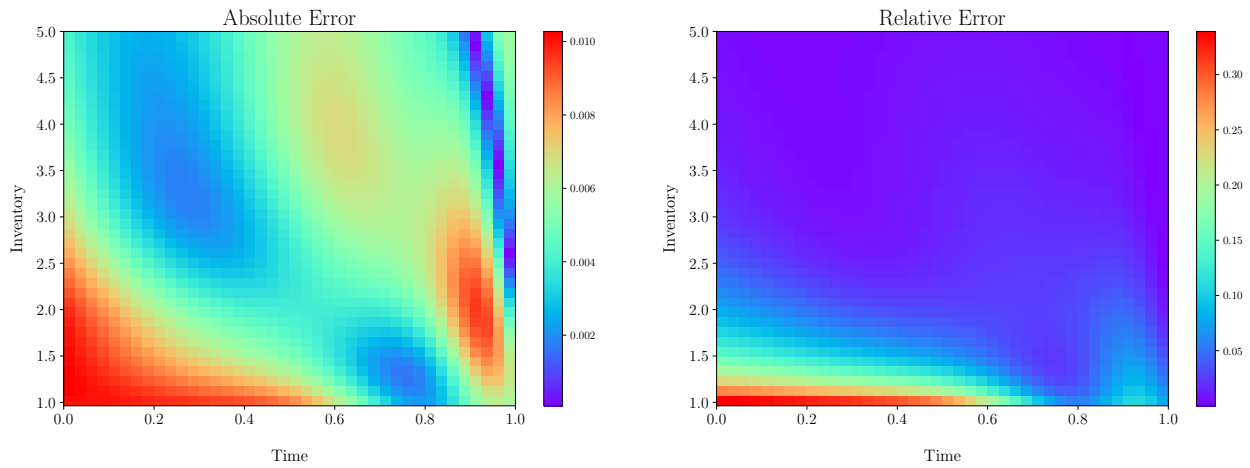


Figure 5.4: Absolute (left panel) and relative (right panel) error in the value function of the optimal execution problem compared to the analytical solution.

where V^i is the value function for agent i ; α^i is the agent's control which is the rate at which bank i borrows from or lends to the central bank; $\mathbf{x} = (x^1, \dots, x^n)$ are the state variables corresponding to the log-monetary reserves for each bank with \bar{x} being the sample mean of this vector; σ and ρ represent the volatility of the log-reserve and the correlation between the noise processes and a common noise process; a is the mean reversion rate in log-reserves; c, q and ϵ are preference parameters related to various running and terminal penalties. It is possible to arrive at a simplified system of HJB equations that do not contain an optimization step, given as follows:

$$\begin{cases} \partial_t V^i + \sum_{j=1}^N [a(\bar{x} - x^j) - \partial_j V^j] \partial_j V^i + \frac{\sigma^2}{2} \sum_{j,k=1}^N (\rho^2 + \delta_{jk}(1 - \rho^2)) \partial_{jk} V^i \\ \quad + \frac{1}{2}(\epsilon - q)^2 (\bar{x} - x^i)^2 + \frac{1}{2} (\partial_i V^i)^2 = 0 \\ V^i(T, \mathbf{x}) = \frac{c}{2} (\bar{x} - x^i)^2 \end{cases} \quad Ex \quad (5.2)$$

for $i = 1, \dots, n$.

Remarkably, this system of PDEs can be solved in closed-form to obtain the value function and the optimal control for each agent:

$$V^i(t, \mathbf{x}) = \frac{\eta(t)}{2} (\bar{x} - x^i)^2 + \mu(t) \quad (5.3a)$$

$$\alpha_t^{i*} = \left(q + \left(1 - \frac{1}{N}\right) \cdot \eta(t) \right) (\bar{X}_t - X_t^i) \quad (5.3b)$$

$$\text{where } \eta(t) = \frac{-(\epsilon - q)^2 \left(e^{(\delta^+ - \delta^-)(T-t)} - 1 \right) - c \left(\delta^+ e^{(\delta^+ - \delta^-)(T-t)} - \delta^- \right)}{(\delta^- e^{(\delta^+ - \delta^-)(T-t)} - \delta^+) - c \left(1 - \frac{1}{N^2}\right) \left(e^{(\delta^+ - \delta^-)(T-t)} - 1 \right)}$$

$$\mu(t) = \frac{1}{2} \sigma^2 (1 - \rho^2) \left(1 - \frac{1}{N}\right) \int_t^T \eta(s) ds$$

$$\delta^\pm = -(a + q) \pm \sqrt{R}, \quad R = (a + q)^2 + \left(1 - \frac{1}{N^2}\right) (\epsilon - q)^2$$

We apply the DGM algorithm² to the system (5.1) for the three-player ($N = 3$) case with correlation $\rho = 0.5$, $\sigma = 0.2$, $a = 1$, $q = 1$, $\epsilon = 10$, $c = 1$, and $T = 1$ and compare the results with the analytical solution (5.3). The plots for these results are given in Figures 5.5 to 5.10. The modified DGM could be applied in this case with some additional computational cost.

²Note that this problem requires computing second-order derivatives which can be computationally costly. We outline an alternative procedure that we use to compute the Hessian in Appendix B.

Player 3 Inventory - $X_3 = 2.00$

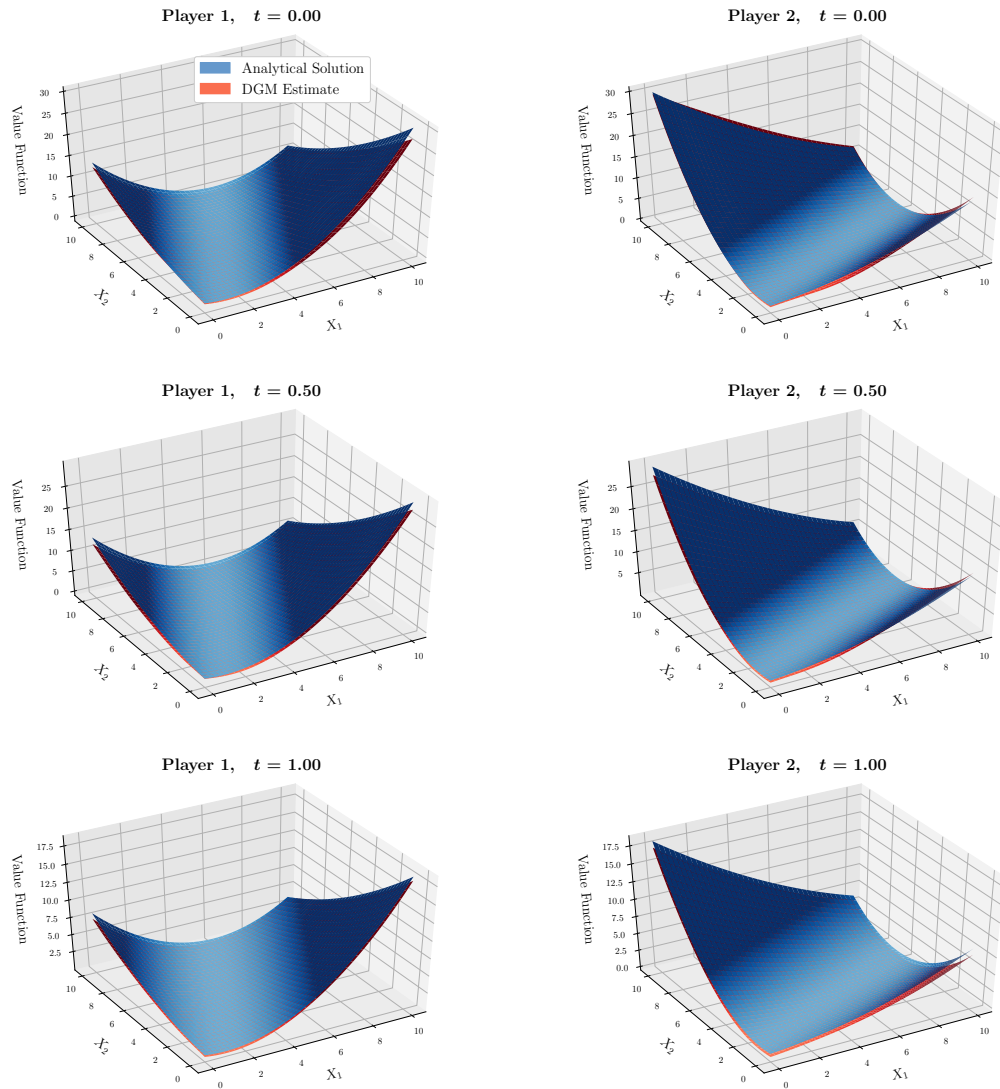


Figure 5.5: Value function of players 1 and 2 at different times in the 3-player systemic risk problem when inventory of player 3 is equal to 2.

Player 3 Inventory - $X_3 = 5.00$

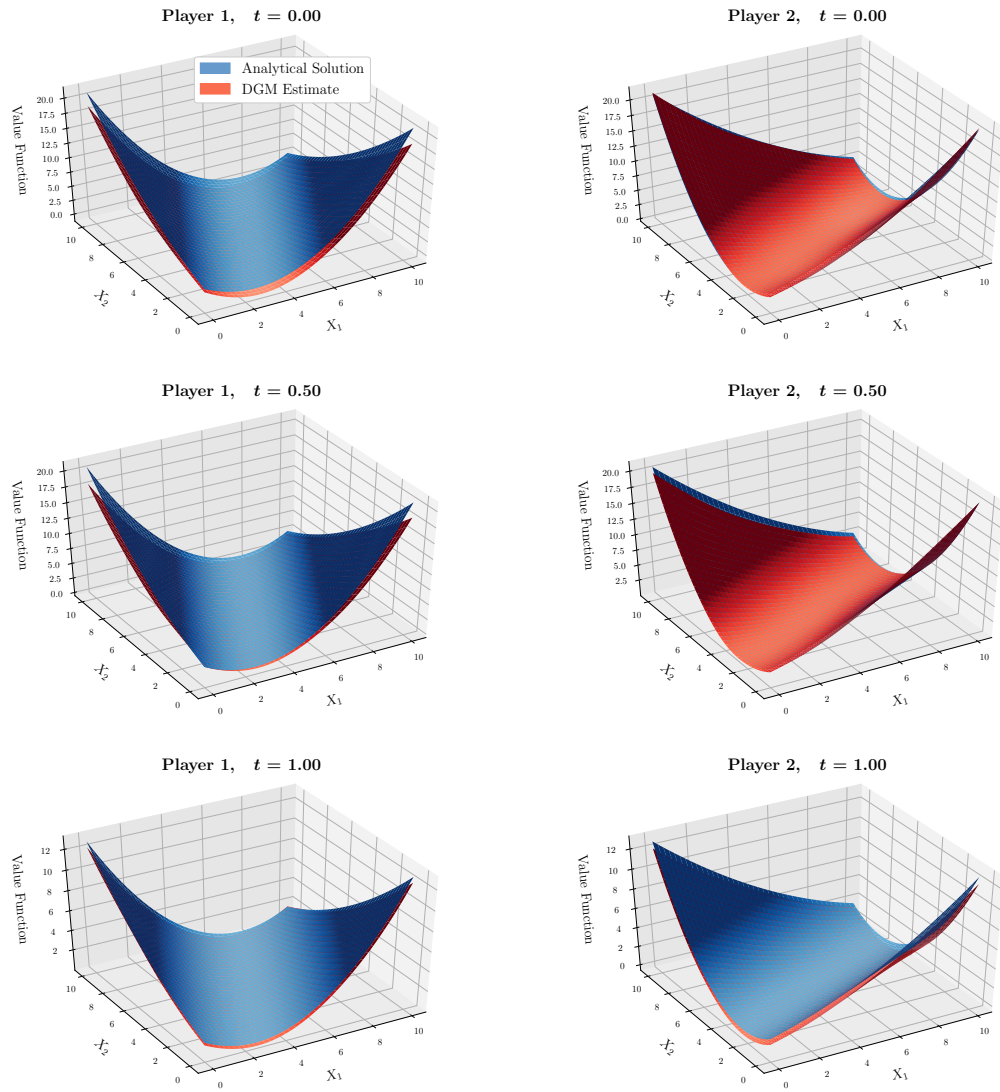


Figure 5.6: Value function of players 1 and 2 at different times in the 3-player systemic risk problem when inventory of player 3 is equal to 5.

Player 3 Inventory - $X_3 = 2.00$

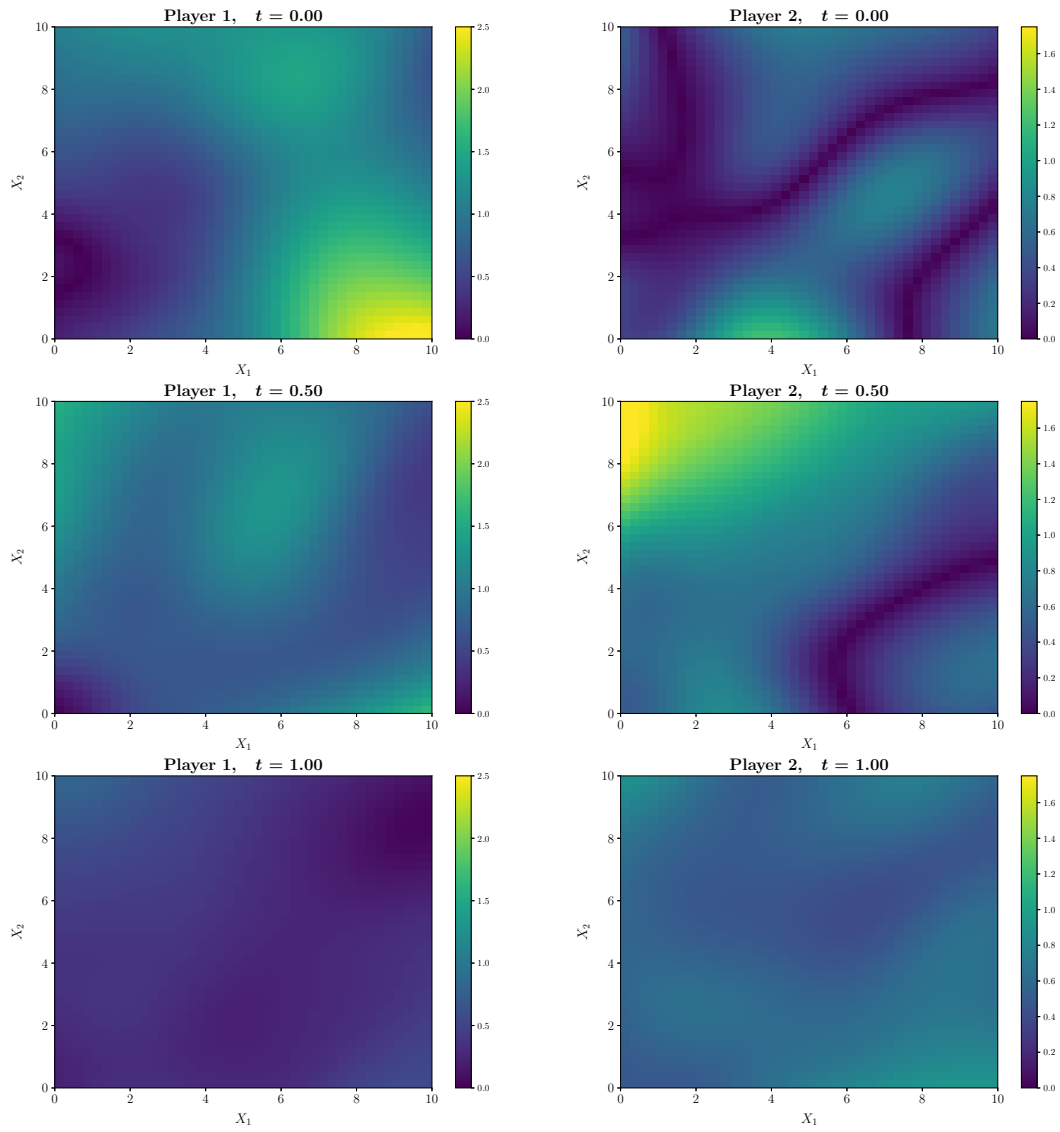


Figure 5.7: Absolute errors in value function of players 1 and 2 at different times in the 3-player systemic risk problem when inventory of player 3 is equal to 2.

Player 3 Inventory - $X_3 = 5.00$

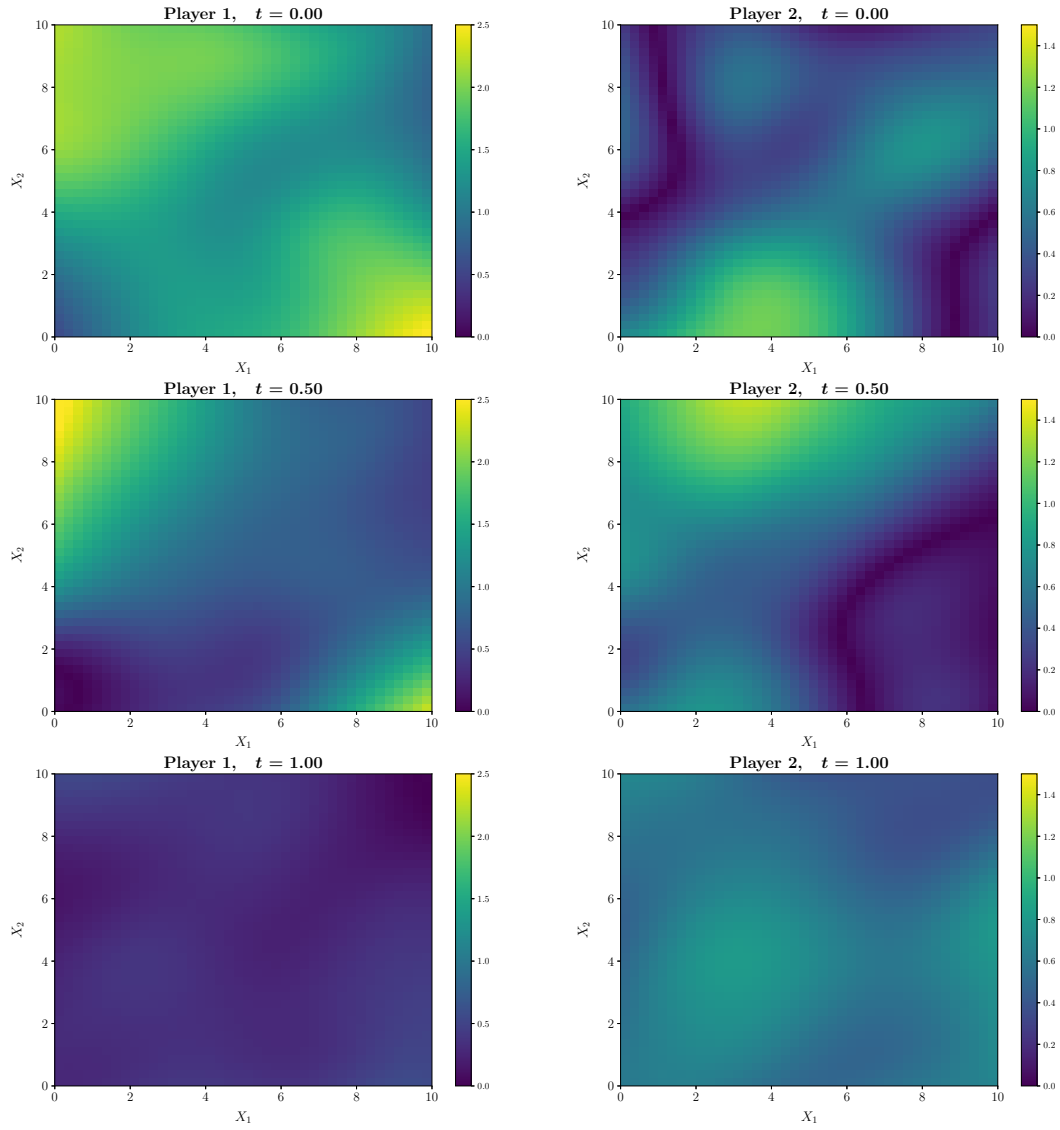


Figure 5.8: Absolute errors in value function of players 1 and 2 at different times in the 3-player systemic risk problem when inventory of player 3 is equal to 5.

Player 3 Inventory - $X_3 = 2.00$

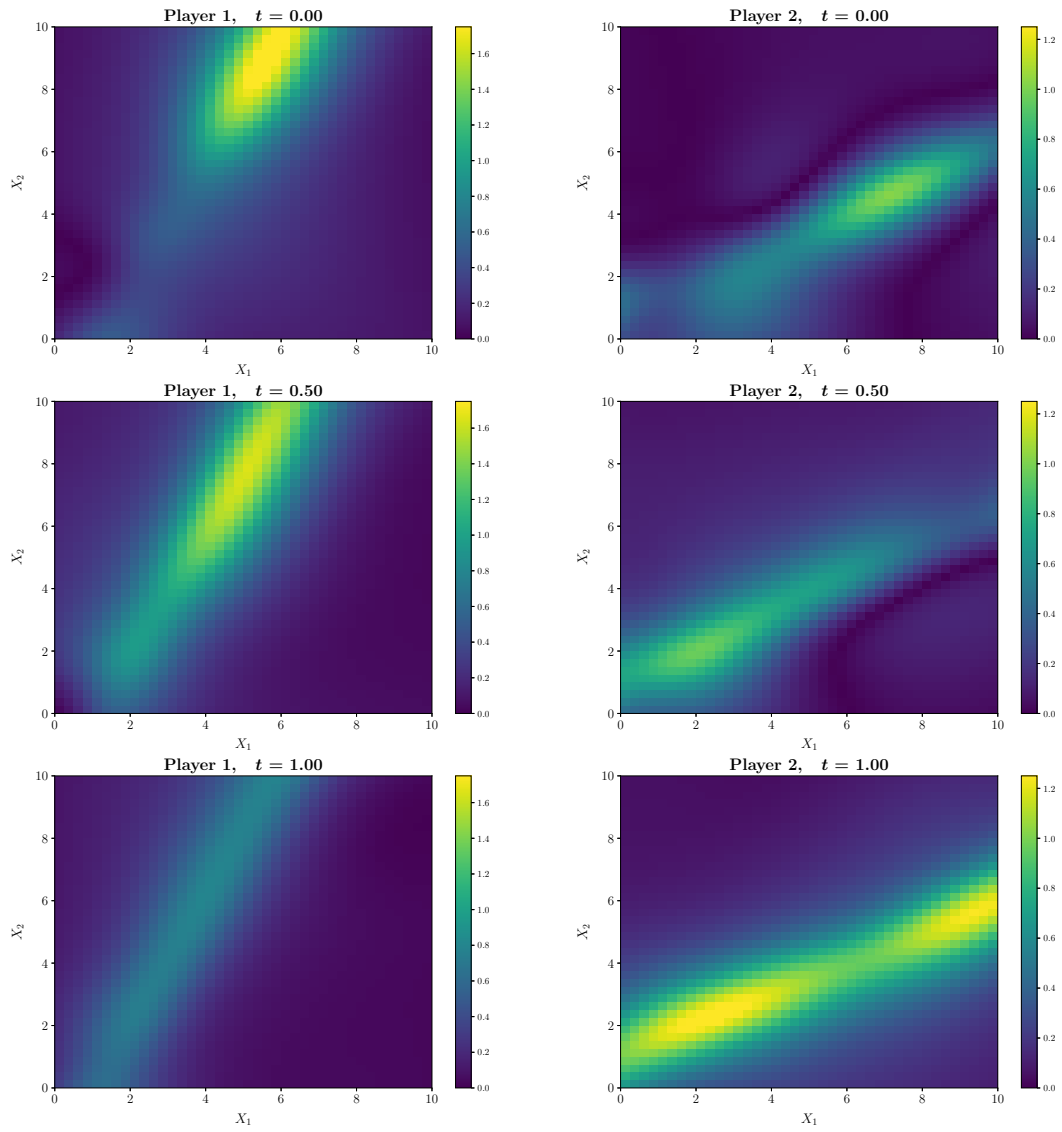


Figure 5.9: Relative errors in value function of players 1 and 2 at different times in the 3-player systemic risk problem when inventory of player 3 is equal to 2.

Player 3 Inventory - $X_3 = 5.00$

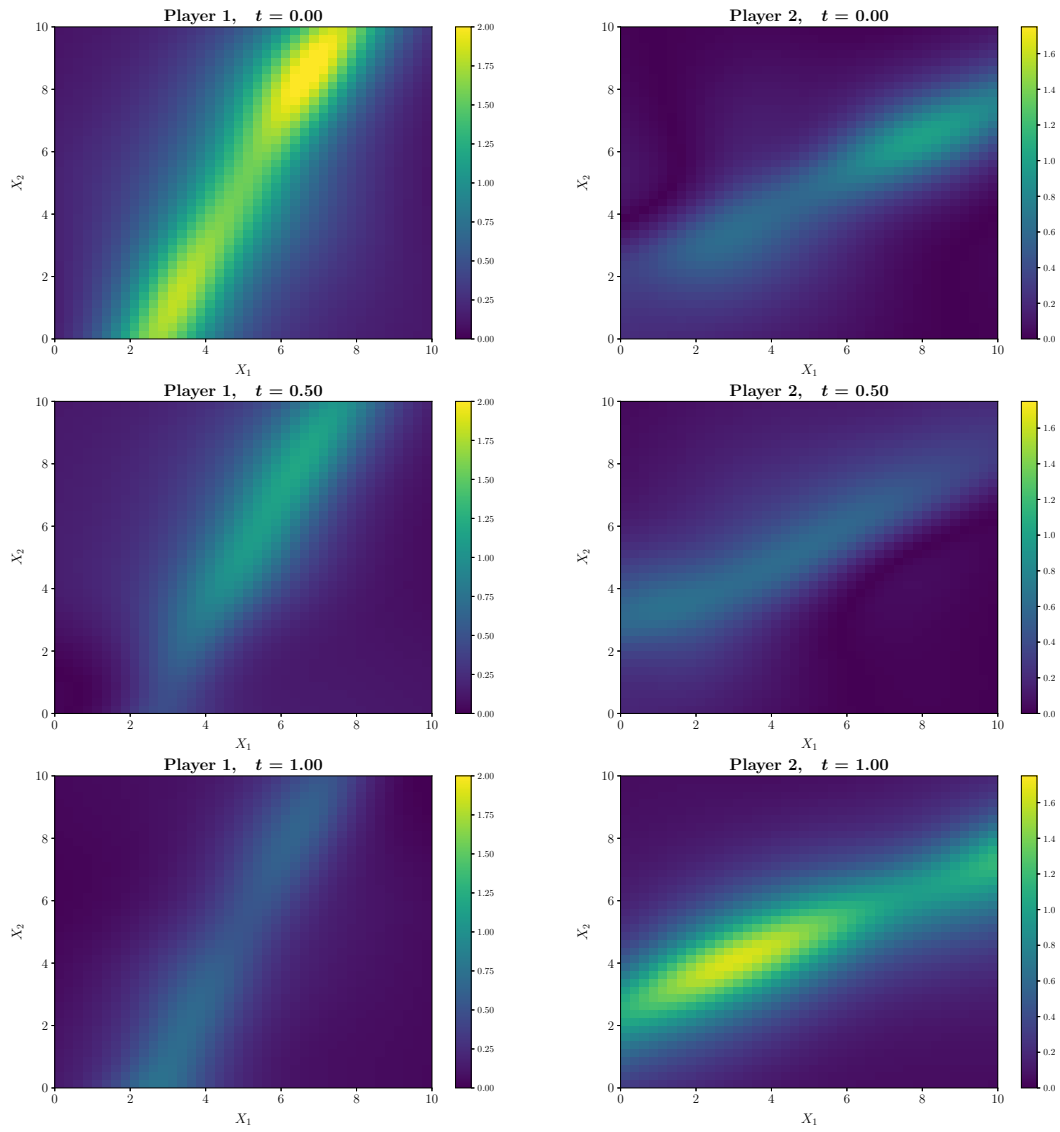


Figure 5.10: Relative errors in value function of players 1 and 2 at different times in the 3-player systemic risk problem when inventory of player 3 is equal to 5.

6. Mean Field Games

The final application we consider is based on the work of Cardaliaguet and Lehalle (2017) in the context of mean field games (MFGs), where the interest is in modeling the behavior of a large number of small interacting market participants. Building on the optimal execution problem discussed in Section 4.3 of this paper, Cardaliaguet and Lehalle (2017) propose extensions in a number of directions. First, traders are assumed to be part of a mean field game and the price of the underlying asset is impacted permanently, not only by the actions of an individual agent, but by the aggregate behavior of all agents acting in an optimal manner. In addition to this aggregate permanent impact, an individual trader faces the usual temporary impact effects of trading too quickly. The other extension is to allow for varying preferences among the traders in the economy. That is, traders may have different tolerance levels for the size of their inventories both throughout the investment horizon and at its end. Intuitively, this framework can be thought of as the agents attempting to “trade optimally within the crowd.”

This application is of particular interest to us since it consists of both a system of HJB equations describing the optimal control problem of each individual agent along with a Fokker-Planck equation which governs the dynamics of the aggregate behavior of all agents. This forces us to combine the techniques of used in Sections 3 and 4 in order to apply the DGM algorithm effectively.

Now, the HJB-Fokker-Planck system associated with the mean field game problem is:

$$\left\{ \begin{array}{l} -\alpha\mu_t q = \partial_t h^a - \phi^a q^2 + \sup_{\nu \in \mathcal{A}} \left\{ \nu \partial_q h^a - \kappa \nu^2 \right\} = 0 \\ h^a(T, x, S, q; \mu) = A^a q^2 \\ \partial_t m + \partial_q \left(m \nu^a(t, q) \right) = 0 \\ m(0, q, a) = m_0(q, a) \\ \mu_t = \int_{(q,a)} \nu^a(t, q) m(t, q, a) dq da \quad \text{and} \quad \nu^a(t, q) = \frac{\partial_q h^a(t, q)}{2\kappa} \end{array} \right. \quad (6.1)$$

The first two lines of system above correspond to the HJB equation associated with the optimal control problem faced by agent a . The variables in these equations are identical to the optimal execution discussed in Section 4.3 with the addition of superscripts to indicate the association with a particular agent and the state variable μ which corresponds to net sum of the trading rates of all agents and the parameter κ which reflects the linear price sensitivity to this aggregate activity. The next three lines capture the evolution of the distribution of inventories across agents $m(t, q, a)$ and how this is driven by the net flow μ_t which in turn given by the aggregation of all agents' actions. The evolution of the density m , which begins at $m_0(q, a)$, through time is governed by a Fokker-Planck equation, and must also remain positive and integrate to unity. Notice that the Fokker-Planck PDE in principle requires us to know the formula of the Hamiltonian of the HJB equation. Therefore, it is not straightforward how the modified DGM presented in Section 4 should be adjusted in order to applied to the system above. We leave this for future work.

In the sequel we will assume identical preferences $\alpha^a = \alpha, \phi^a = \phi, m_0(q, a) = m_0(q)$, which allows us to find a closed-form solution to this PDE system. The form of the solution is fairly involved so we refer the interested reader to the details in Cardaliaguet and Lehalle (2017). The paper also derives a closed-form expression for the expected inventory across agents through time, $E_t = \int_{(q,a)} q m(t, dq, da)$. We will use both the value function, optimal control and expected inventory to assess the accuracy of our numerical solutions.

In order to apply the DGM algorithm we need to use the techniques discussed in Section 3 to derive modified equations for the inventory density component that guarantees the numerical solution will be positive and integrate to 1. Using the same idea of exponentiating and normalizing used in Section 3 and detailed in Appendix A, we rewrite the density $m(t, q) = \frac{1}{c(t)} e^{-u(t,q)}$. Replacing the resulting PDE for the function u , the system for the MFG in the problem of Cardaliaguet and Lehalle (2017) becomes

$$\left\{ \begin{array}{l} -\alpha \mu_t q = \partial_t h - \phi q^2 + \frac{(\partial_q h)^2}{4\kappa} = 0 \\ h(T, q; \mu) = Aq^2 \\ \partial_t u + \frac{1}{2\kappa} (h \partial_q u - \partial_{qq} h) - \int_{\mathbb{R}} \frac{e^{-u(t,q)}}{\int_{\mathbb{R}} e^{-u(t,y)} dy} \partial_t u(t, q) dq = 0 \\ u(0, q) = \log(m_0(q)c(0)) \\ \mu_t = \int_q \nu(t, q) m(t, q) dq \text{ and } \nu(t, q) = \frac{\partial_q h(t, q)}{2\kappa} \end{array} \right. \quad (6.2)$$

We apply the DGM algorithm to solve the system (6.2) with both integral terms being handled by *importance sampling* as in the Fokker-Planck equation with exponential transformation in Section 3. The system is solved numerically with parameters $A, \phi, \alpha, k = 1$ and with terminal time $T = 1$. The initial mass distribution is taken to be a normal distribution with mean $E_0 = 5$ and variance 0.25. The value function, optimal control along with the expected values of the mass through time were compared with their respective analytical solutions (an analytical solution for the probability mass is not available; however the expected value of this distribution can be computed analytically). The resulting plots can be found in Figures 7.1 to 7.6.

7. Conclusions

In this paper we presented an extension of the Deep Galerkin Method that uses ideas from policy improvement algorithms to solve HJB equations as well as PDEs involving constrained functions. The modified algorithm involves representing the value function and the optimal control as deep neural networks that are trained by taking alternating stochastic gradient descent steps. The algorithm is successfully applied to a number of optimal control problems that arise in financial contexts.

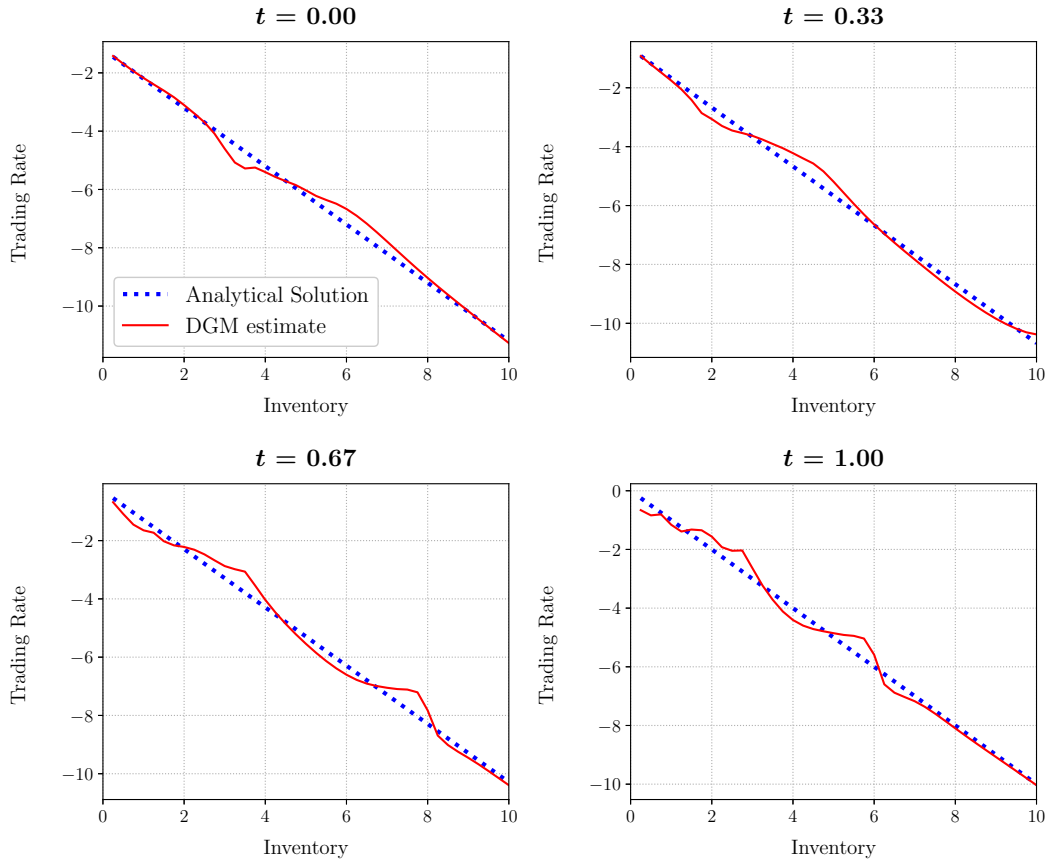


Figure 7.1: Optimal control for the MFG problem at different times.

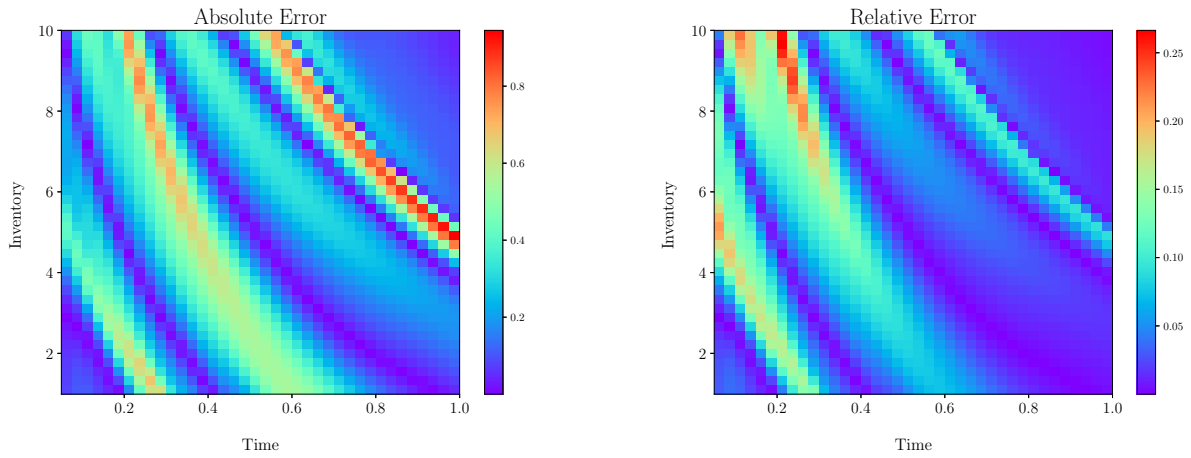


Figure 7.2: Absolute (left panel) and relative (right panel) error in the optimal control of the optimal execution problem compared to the analytical solution.

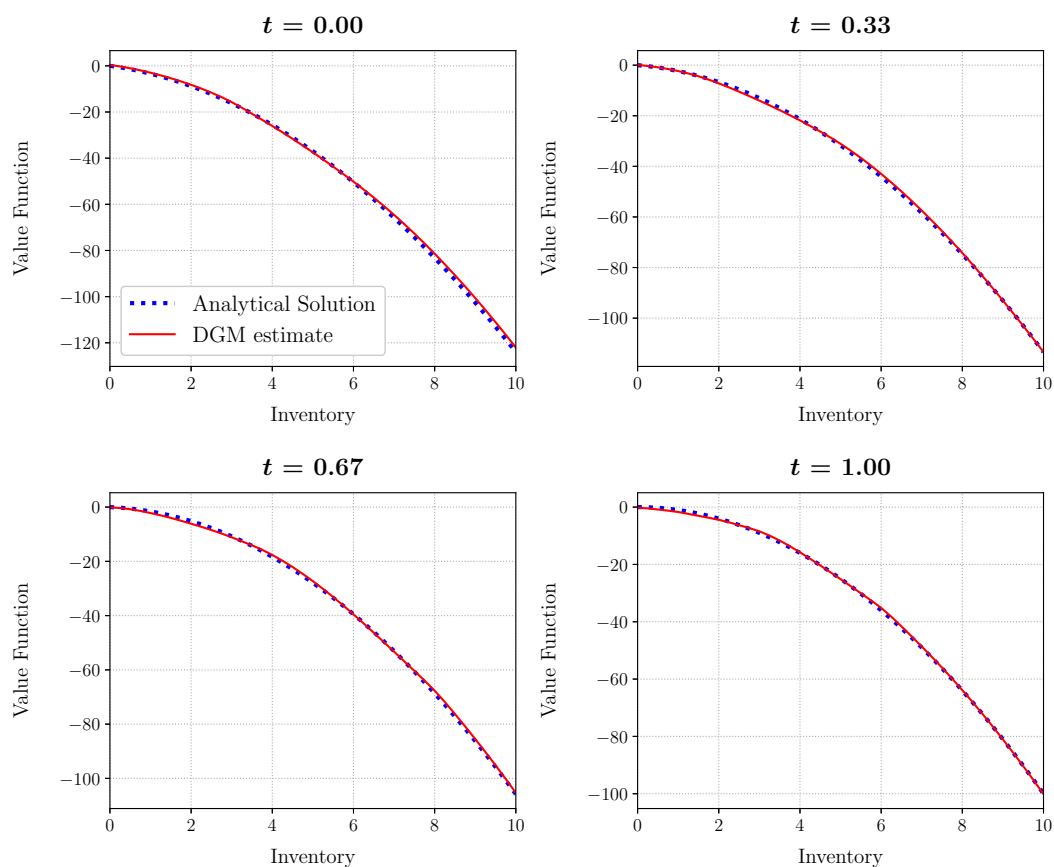


Figure 7.3: Value function for the MFG problem at different times.

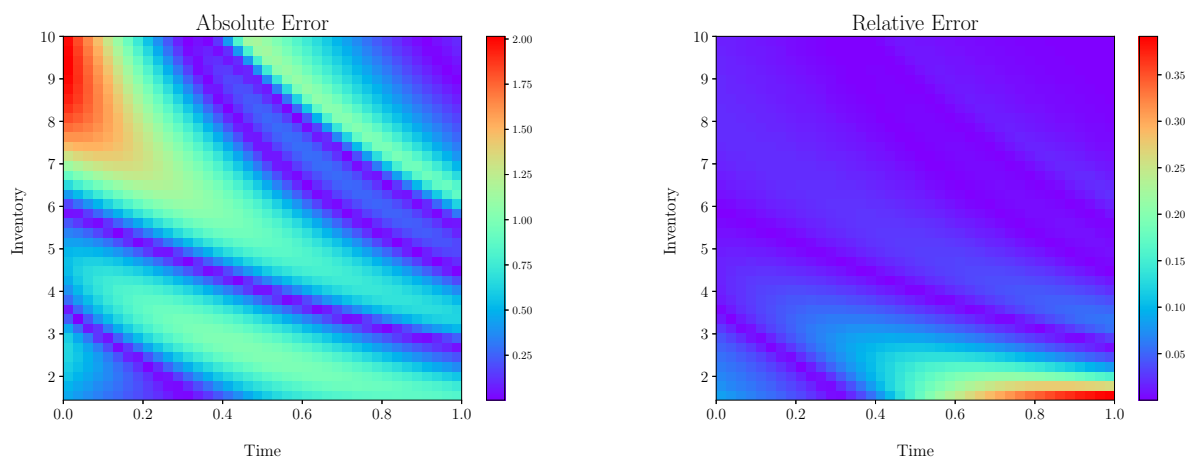


Figure 7.4: Absolute (left panel) and relative (right panel) error in the value function of the optimal execution problem compared to the analytical solution.

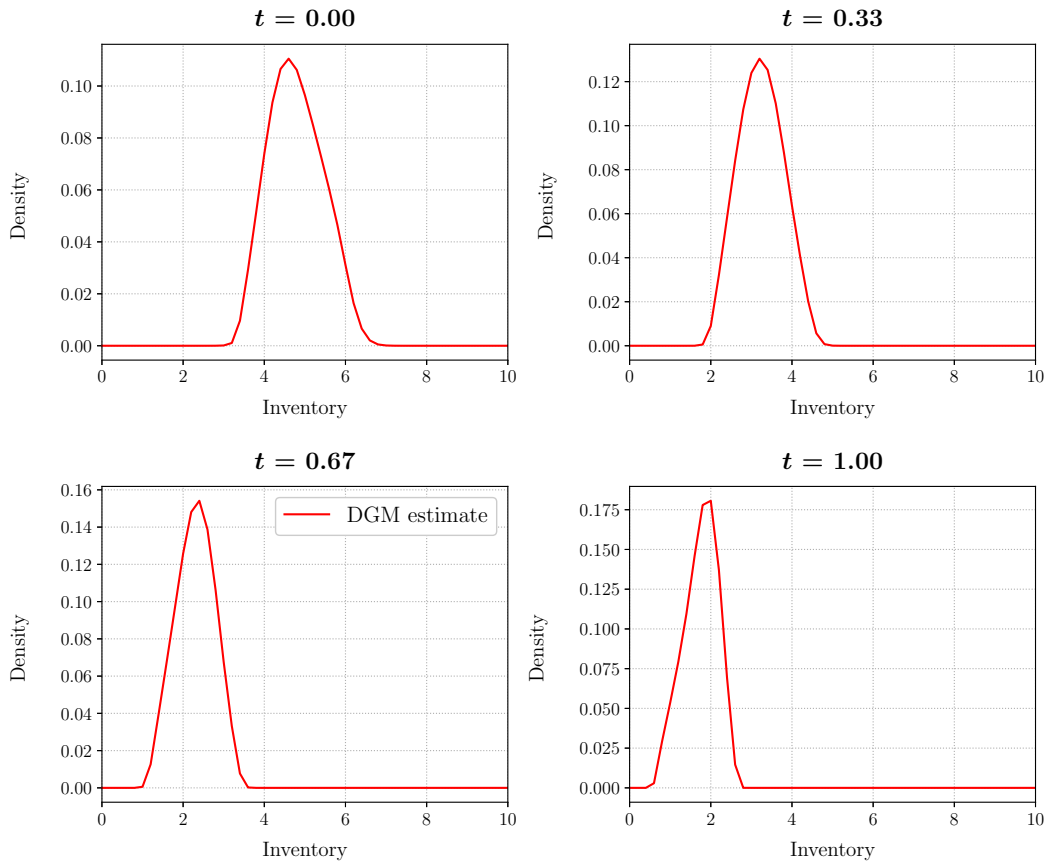


Figure 7.5: Distribution of agents' inventories at different times in the MFG problem.

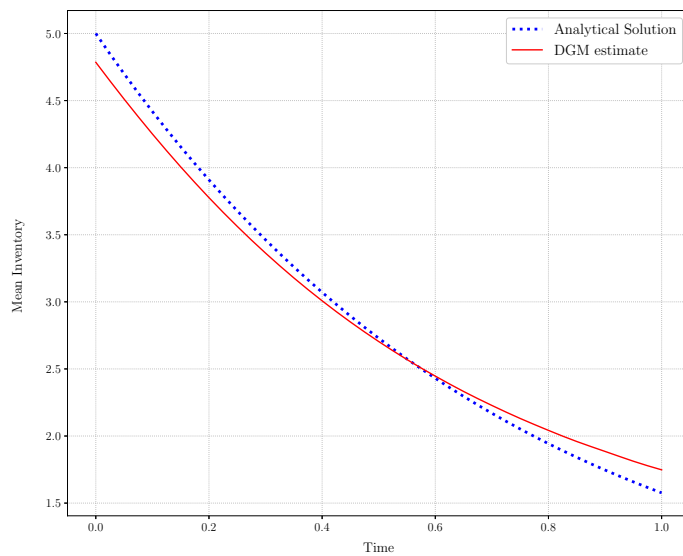


Figure 7.6: Mean inventory across agents through time for the MFG problem.

Appendix A. Reparameterization of the Fokker-Planck Equation

The density function $p(t, x)$ satisfies the PDE

$$\begin{cases} \partial_t p + \partial_x (\mu(x) p(t, x)) + \frac{1}{2} \partial_{xx} (\sigma^2(x) p(t, x)) = 0 & (t, x) \in \mathbb{R}_+ \times \mathbb{R} \\ p(0, x) = f(x) \end{cases}$$

Writing the density function in the following form

$$p(t, x) = \frac{e^{-u(t, x)}}{c(t)} \quad \text{where } c(t) = \int_{\mathbb{R}} e^{-u(t, x)} dx$$

we can find the derivatives of p in terms of u and c :

$$\begin{aligned} \partial_t p &= -\frac{e^{-u(t, x)} \partial_t u}{c(t)} - \frac{c'(t) e^{-u(t, x)}}{c(t)^2} \\ \partial_x p &= -\frac{e^{-u(t, x)} \partial_x u}{c(t)} \\ \partial_{xx} p &= \frac{e^{-u(t, x)} (\partial_x u)^2 - e^{-u(t, x)} \partial_{xx} u}{c(t)} \end{aligned}$$

where the time derivative of c is given by

$$c'(t) = - \int_{\mathbb{R}} \partial_t u(t, x) e^{-u(t, x)} dx.$$

We also have that

$$\begin{aligned} \partial_x (\mu(x) p(t, x)) &= p(t, x) \partial_x \mu + \mu(x) \partial_x p \\ \partial_{xx} (\sigma^2(x) p(t, x)) &= p(t, x) \partial_{xx} \sigma^2 + 2 \partial_x \sigma^2 \partial_x p + \sigma^2(x) \partial_{xx} p \end{aligned}$$

Substituting these terms into the PDE given at the outset and simplifying yields

$$\partial_t u - \partial_x \mu + \mu(x) \partial_x u - \frac{1}{2} \left[\partial_{xx} \sigma^2 - 2 \partial_x \sigma^2 \partial_x u + \sigma^2(x) \left((\partial_x u)^2 - \partial_{xx} u \right) \right] - \frac{\int_{\mathbb{R}} e^{-u(t, x)} \partial_t u dx}{\int_{\mathbb{R}} e^{-u(t, x)} dx} = 0.$$

Finally, the initial condition can be obtained by noticing that

$$p(0, x) = \frac{e^{-u(0, x)}}{c(0)} = f(x) \quad \implies \quad u(0, x) = -\ln(f(x)c(0)),$$

where $c(0)$ could be chosen to be any constant.

Appendix B. Hessian Implementation

Second-order differential equations call for the computation of second derivatives. In principle, given a deep neural network $f(t, \mathbf{x}; \boldsymbol{\theta})$, the computation of higher-order derivatives by automatic differentiation is possible. However, given $\mathbf{x} \in \mathbb{R}^n$ for $n > 1$, the computation of those derivatives becomes computationally

costly, due to the quadratic number of second derivative terms and the memory-inefficient manner in which the algorithm computes this quantity for larger mini-batches. For this reason, we implement a finite difference method for computing the Hessian. In particular, for each of the sample points \mathbf{x} , we compute the value of the neural network and its gradients at the points $\mathbf{x} + h\mathbf{e}_j$ and $\mathbf{x} - h\mathbf{e}_j$, for each canonical vector \mathbf{e}_j , where h is the step size, and estimate the Hessian by central finite differences, resulting in a precision of order $\mathcal{O}(h^2)$. The resulting matrix H is then symmetrized by the transformation $0.5(H + H^T)$.

References

- Achdou, Y. and O. Pironneau (2005). *Computational methods for option pricing*, Volume 30. Siam.
- Al-Aradi, A., A. Correia, D. Naiff, G. Jardim, and Y. Saporito (2018). Solving nonlinear and high-dimensional partial differential equations via deep learning. *arXiv preprint arXiv:1811.08782*.
- Almgren, R. and N. Chriss (2001). Optimal execution of portfolio transactions. *Journal of Risk* 3, 5–40.
- Beck, C., S. Becker, P. Cheridito, A. Jentzen, and A. Neufeld (2019). Deep splitting method for parabolic pdes. *arXiv preprint arXiv:1907.03452*.
- Brandimarte, P. (2013). *Numerical methods in finance and economics: a MATLAB-based introduction*. John Wiley & Sons.
- Burden, R. L., J. D. Faires, and A. C. Reynolds (2001). *Numerical analysis*. Brooks/cole Pacific Grove, CA.
- Cardaliaguet, P. and C.-A. Lehalle (2017). Mean field game of controls and an application to trade crowding. *Mathematics and Financial Economics*, 1–29.
- Carmona, R., L.-H. Sun, and J.-P. Fouque (2015). Mean field games and systemic risk. *Communications in Mathematical Sciences* 14(4), 911–933.
- Cartea, Á. and S. Jaimungal (2015). Optimal execution with limit and market orders. *Quantitative Finance* 15(8), 1279–1291.
- Cartea, Á. and S. Jaimungal (2016). Incorporating order-flow into optimal execution. *Mathematics and Financial Economics* 10(3), 339–364.
- Cartea, Á., S. Jaimungal, and J. Penalva (2015). *Algorithmic and high-frequency trading*. Cambridge University Press.
- E, W., J. Han, and A. Jentzen (2017). Deep learning-based numerical methods for high-dimensional parabolic partial differential equations and backward stochastic differential equations. *Communications in Mathematics and Statistics* 5(4), 349–380.
- E, W., M. Hutzenthaler, A. Jentzen, and T. Kruse (2016). Multilevel Picard iterations for solving smooth semilinear parabolic heat equations.

- E, W., M. Hutzenthaler, A. Jentzen, and T. Kruse (2019). On multilevel Picard numerical approximations for high-dimensional nonlinear parabolic partial differential equations and high-dimensional nonlinear backward stochastic differential equations. *Journal of Scientific Computing* 79(3), 1534–1571.
- Han, J., A. Jentzen, and W. E (2018). Solving high-dimensional partial differential equations using deep learning. *Proceedings of the National Academy of Sciences* 115(34), 8505–8510.
- Hochreiter, S. and J. Schmidhuber (1997). Long short-term memory. *Neural computation* 9(8), 1735–1780.
- Huré, C., H. Pham, and X. Warin (2019). Some machine learning schemes for high-dimensional nonlinear pdes. *arXiv preprint arXiv:1902.01599*.
- Hutzenthaler, M., A. Jentzen, T. Kruse, and T. A. Nguyen (2019). A proof that rectified deep neural networks overcome the curse of dimensionality in the numerical approximation of semilinear heat equations.
- Hutzenthaler, M., A. Jentzen, and P. von Wurstemberger (2019). Overcoming the curse of dimensionality in the approximative pricing of financial derivatives with default risks.
- Ito, K., C. Reisinger, and Y. Zhang (2019). A neural network based policy iteration algorithm with global H^2 -superlinear convergence for stochastic games on domains. *arXiv preprint arXiv:1906.02304*.
- Jacka, S. D. and A. Mijatović (2017). On the policy improvement algorithm in continuous time. *Stochastics* 89, 348–359.
- Merton, R. (1971). Optimum consumption and portfolio-rules in a continuous-time framework. *Journal of Economic Theory*.
- Merton, R. C. (1969). Lifetime portfolio selection under uncertainty: The continuous-time case. *The Review of Economics and Statistics*, 247–257.
- Sirignano, J. and K. Spiliopoulos (2018). DGM: A deep learning algorithm for solving partial differential equations. *Journal of Computational Physics* 375, 1339–1364.
- Srivastava, R. K., K. Greff, and J. Schmidhuber (2015). Highway networks. *arXiv preprint arXiv:1505.00387*.